DOE/JPL-1060-62
(DE84009157)

SOLAR TESTS OF APERTURE PLATE MATERIALS FOR SOLAR THERMAL DISH COLLECTORS

By
L. D. Jaffe

August 15, 1983

Work Performed Under Contract No. AT04-81AL16228

Jet Propulsion Laboratory
California Institute of Technology
Pasadena, California

DISCLAIMER

Solar Tests of Aperture Plate Materials for Solar Thermal Dish Collectors

L.D. Jaffe

August 15, 1983

ABSTRACT

In parabolic dish solar collectors, walk-off of the spot of concentrated
sunlight can be a hazard if a malfunction causes the concentrator to stop
following the sun. Therefore, a test program was carried out to evaluate the
behavior of various ceramics, metals, and polymers under solar irradiation of
about 7000 kW/m^2 (peak) for 15 minutes. The only materials that did not
slump or shatter were two grades of medium-grain extruded graphite.
High-purity, slip-cast silica might be satisfactory at somewhat lower flux.
Oxidation of the graphite appeared acceptable during tests simulating
walk-off, acquisition (2000 cycles on/off sun), and spillage (continuous
on-sun operation).

ACKNOWLEDGMENTS

CONTENTS

Figures

Tables

EXECUTIVE SUMMARY

In parabolic dish solar collectors, walk-off of the spot of concentrated sunlight can be a hazard if a malfunction causes the concentrator to stop following the sun. The use of protective materials that can withstand exposure to walk-off conditions without active cooling provides certain advantages. A test program, therefore, was carried out to evaluate behavior of materials under simulated walk-off conditions. Each test consisted of exposure to concentrated sunlight at a peak flux density of about 7000 kW/m^2 for 15 minutes. For material that appeared promising in these tests, additional tests were conducted to evaluate behavior under conditions simulating other conditions of solar exposure that receiver aperture plates must often withstand in dish collectors: solar acquisition and solar spillage.

Types of materials tested under simulated walk-off conditions included graphite, silicon carbide, silica, various silicates, alumina, zirconia, aluminum, copper, steel, and polytetrafluoroethylene. Of these, the only material that neither cracked nor melted was grade G-90 graphite, a premium grade. Grade CS graphite, a lower cost commercial grade, cracked half-way across, but did not fall apart. With proper design, this grade should probably perform satisfactorily as a receiver aperture plate. Both of these grades are medium-grain extruded graphites. A graphite cloth (graphitized polyacrylonitrile) showed fair performance when tested as a single thin ply; it might be useful as a multi-ply assembly.

The only other material tested which appeared promising was high-purity slip-cast silica; samples survived from one and one-half to four minutes. This duration is inadequate for walk-off protection, but the material might well be satisfactory at flux densities somewhat lower than those used in these tests.

The other grades of graphite and silica tested, and all the samples of alumina, zirconia, silicates, silicon carbide, aluminum, copper, steel, and polytetrafluoroethylene, either melted or fractured quickly during the walk-off tests.

Coatings of white high-temperature paint or boron nitride did not improve the performance of graphite samples. Immersion in water prior to test, simulating rain, did not affect their performance.

Oxidation of grades CS and G-90 graphite per 15-minute simulated walk-off varied from 0.2 to 8 mm (0.008 to 0.3 in.) of thickness, from 2 to 22% of the mass [normalized to 25 mm (1 in.) thickness]. This will probably be acceptable for many applications. The amount of oxidation varied strongly with the wind speed.

Grade CS graphite was tested for up to 2000 cycles simulating 1-second periods of acquisition at the same flux density as the walk-off test. Loss in 2000 cycles at moderate to high winds was about 5 mm in thickness or 0.15% of the sample mass; this appears to be tolerable. Tests under simulated spillage conditions were limited to measurements of the temperature of the lip of a simulated aperture plate of grade CS graphite. They indicate that at spillage levels up to 2% the lip temperature would be below 250°C (480°F), low enough to provide adequate lifetime of this material with respect to oxidation.

SECTION I

INTRODUCTION

In a solar thermal dish-type power plant, sunlight is focused by a concentrator (or "dish") onto a receiver where it is absorbed and its energy transferred to heat a working fluid. The hot fluid may be utilized directly or may go to a heat engine, which converts the thermal energy to mechanical; the engine may in turn drive a generator to produce electricity. The plant may include one or more collectors, each consisting of a concentrator with a receiver mounted near its focus. Concentrators are typically 5 to 15 m (16 to 60 ft) in diameter, with focal ratios of 0.5 to 1. Receivers are usually cavity type, with the concentrated sunlight entering through an aperture. In operation, each concentrator is pointed at the sun and follows its motion, turning about two axes.

If a malfunction occurs while a concentrator is pointed at the sun, motion of the concentrator may stop. As the sun moves relative to the Earth, the spot of concentrated sunlight then slowly "walks off" the receiver aperture, across the receiver face plate, and perhaps, depending on the design, across adjacent portions of the concentrator. Intense local heating by the concentrated sunlight may damage or destroy these parts and put the unit out of service.

A wide variety of methods may be used for protection against damage by walk-off. They include materials that can withstand the concentrated sunlight, provision of water-cooling, shutters, or emergency devices to point the concentrator away from the sun, provision of emergency power to turn the concentrator, etc. Advantages and disadvantages of various methods are discussed in Reference 1. Many of the methods require use of emergency mechanisms, power or cooling supplies, and controls; these may add significant complexity and cost and may not function reliably when needed. Use of materials that can withstand the concentrated sunlight without active cooling has the advantage of providing passive protection, which should increase reliability, and may be less costly than alternative techniques. Moreover, a shutter, for example, must itself be made of material able to withstand walk-off heating or must be actively cooled during walk-off.

The "spot" of intense sunlight at the focus is typically 8 to 50 cm (3 to 20 in.) in diameter, though its edge is not sharp. Solar flux density within the spot is usually not uniform, but peaked near the center, and may be approximated by a two-dimensional Gaussian distribution. The peak flux density is typically 1000 to 15,000 kW/m^2. With these inputs, a gray body losing heat only by reradiation may reach an equilibrium temperature of 3750°C (6800°F). Because the spot moves at the Earth's rotation rate of 15 deg/h, typical times for the spot to move its own diameter are 5 to 15 minutes (except in polar regions). For passive protection, a material and design that can withstand these conditions is needed.

Ability to withstand walk-off is only one of the possible requirements for an aperture plate. In most designs, each time the concentrator is swung to point it at or away from the sun during normal operation, the spot of sunlight traverses the aperture plate. (This exposure of the plate can be

avoided if a shutter or other shadowing device is used.) The exposure time during normal sun acquisition or "deacquisition" is much shorter than during walk-off: typically 1 to 2 seconds for the spot to move its own diameter. However, sun acquisition and deacquisition may be expected once or several times a day when the concentrator is operating, whereas walk-off occurs only through malfunction. For reasonable lifetime, an aperture plate that is exposed to the sun during acquisition should withstand many cycles of acquisition and deacquisition.

An additional requirement of any aperture plate is that it must withstand "spillage": the fraction of the concentrated sunlight that does not pass into the receiver aperture when the collector is pointed at the sun, but is instead intercepted by the lip of the aperture plate. Spillage occurs because of the diffuse character of the spot edge and because of the pointing errors and structural deflections of the collector that occur during normal operation. (It is not desirable to increase the aperture size to prevent spillage because a larger aperture increases reradiation and convection losses from the receiver and, therefore, lowers collector efficiency.) The flux density at the lip during normal operation is usually from one percent to a few percent of the peak flux density of the spot, but the lip is exposed to this spillage at all times when the concentrator is pointed at the sun.

Some work has been reported on the ability of uncooled materials to withstand concentrated sunlight for short periods of time (References 2 through 9). Except for some limited tests (References 8,9), this prior work was not oriented toward dish concentrators, and either the flux densities or exposure times used for testing were lower than those of interest for walk-off of dish concentrators. It therefore appeared worthwhile to undertake tests to evaluate candidate materials.

In particular, impetus for this work came from JPL interest in finding a suitable aperture plate material for passive protection for the organic Rankine system developed under contract with JPL by the Ford Aerospace and Communications Corporation (FACC) (References 10,11). In this system, the peak flux density at the receiver aperture under design conditions was expected to be about 7,000 kW/m^2.

An important constraint on this materials evaluation was cost of the test program, which was severely limited. This in turn limited the choice of materials to be tested and the measurements that could be made.

SECTION II

TYPES OF MATERIALS TESTED

Important requirements for aperture plate materials include the following:

(1)   Ability to withstand a walk-off and preferably several walk-offs. (In principle, replacement after each walk-off might be possible, but this is undesirable because of downtime, cost, nuisance, and poor public image.)

(2)   During walk-off the material should not produce fragments, drops, or smoke that can damage or obscure the concentrator optical surface.

(3)   The material, in a suitable design, should withstand from thousands to tens of thousands of routine sun acquisitions and deacquisitions.

(4)   The material should withstand spillage on the lip of the aperture for tens of thousands of hours.

(5)   Cost of material and labor for each aperture plate should not exceed a few hundred dollars installed, in quantity production.

These requirements lead to the following materials characteristics:

(1)   Very high melting point.

(2)   High resistance to thermal shock. This in turn favors low coefficient of thermal expansion, high thermal conductivity, low modulus of elasticity, and high fracture strength. Ductile behavior would be advantageous.

(3)   Slow rate of oxidation at service temperatures. (This characteristic tends to rule out high-melting metals.) Also, the material should have a slow rate of vaporization and decomposition at service temperatures. (Ablative materials, in general, appear unsuitable because they usually produce drops and smoke in service.)

(4)   Preferably, low solar absorptance.

(5)   Preferably, but less importantly, high thermal emittance at service temperature.

(6)   Preferably, high thermal conductivity (in the direction perpendicular to the concentrator optical axis) in order to spread the absorbed heat.

(7)   Preferably, low weight per unit area, as used.

(8)   Low initial cost, including low fabrication cost and low life-
cycle cost. (This characteristic is extremely important.)

The limited budget for this work meant that samples for testing also
had to be low in cost. Many of the samples were provided free of charge by
interested companies or obtained from JPL surplus.

The general types of materials tested included graphite, silicon
carbide, silica, silicates, alumina, zirconia, steel, and polytetra-
fluoroethylene. Also tested were aluminum and copper with temperature-
resistant coatings, and graphite with temperature-resistant coatings.
Individual samples tested are listed in Tables 2-1 through 2-3 with some
further details. More complete information on each of the materials tested is
given in Appendix A.

The preferred sample size selected was 200 x 200 x 25 mm (8 x 8 x 1 in.)
to have samples large enough when compared to the solar spot size and thick
enough to provide reasonable protection. A few thicker samples were tested to
see if greater thickness improved performance. Because many samples were
provided free of charge rather than purchased, they were often smaller than
preferred. Some were as thin as 0.4 mm (0.017 in.); these samples were
provided more because of the supplier's interest in using them for protection
during normal operation, acquisition, and deacquisition than for possible
walk-off protection.

For spillage tests, one edge of the sample was tapered and rounded. Two
thermocouples were inserted in each spillage test sample with their junctions
close to the tapered edge (Figures 2-1 and 2-2).

Each sample was identified with a sample number, as shown in the tables.
When a sample was retested, a slash and digit (/2, for example) was appended
to the sample number.

Table 2-1. Solar Walf-Off Tests: Materials and Test Results

Material and Type	Sample No.	Notes	Bulk Density, g/cm³	Approx. Reflectance	Thickness	Approx. Width	Approx. Height	Mass before Test, g	Insolation during Test, W/m²	Wind Speed during Test, m/s	Time, min:sec	Nature	Duration of Test, min:sec	Thickness, mm	Mass, %	Test No.
Graphite																
3499	3499-1	–	1.67	0.09	26.0	204	204	1784	660	2	1:15	Cracked apart	1:35	0.5	0.5	J-2
	3499-2	1	1.67	0.9	25.7	204	204	1779	700	3	8:20	Shattered	8:20	0.4	0.4	20
8826	8826-1	–	1.72	0.09	25.7	204	204	1844	580	3	1:10	Shattered	1:15	0.6	0.6	3
	8826-2	2	1.72	0.9	25.7	204	204	1843	730	2	1:30	Shattered	1:30	0.2	0.0	26
CS	HB-1	12,14	1.79	0.1	36.2	153	203	1795	790	1	2:35	Cracked halfway	2:40	~0.3	1.6	14
	HB-1/2	11,14	–	–	35.9	153	203	1767	840	5	–	None	14:00	7.9	8.5	24
	CS-1	–	1.68	–	28.1	205	205	1980	620	3	8:30	Cracked halfway	9:40	0.4	3.4	1
	CS-1/2	11	–	–	27.7	205	205	1913	830	2	–	None	8:00	2.2	3.2	22
	CS-1/3 & 4	11,15	–	–	25.6	207	207	1852	880	3	–	None	27:20	4.7	13.1	40,42
	CS-2	1	1.68	–	28.1	205	205	1962	820	3	7:55	Cracked through	8:00	0.1	0.8	19
	CS-3	–	1.76	0.09	37.2	207	207	2796	680	7	14:00	Cracked halfway	15:00	~5	9.3	29
	CS-3/2	11	–	–	34.7	207	207	2536	670	11	–	None	15:00	~4	9.8	37
	CS-4	7	1.76	0.1	36.7	207	207	2751	800	10	2:40	Cracked halfway	15:00	~8	9.2	30
	CS-4/2	11	–	–	34.4	207	207	2498	780	9	–	None	15:00	~2	14.1	38
	CS-6	1	1.76	0.8	37.4	207	207	2805	760	5	2:15	Cracked halfway	15:00	2.6	5.2	36
	CS-8	–	1.69	0.1	13.5	204	204	950	670	4	0:10	Cracked halfway	15:00	2.3	15.8	49
	CS-9	–	1.69	0.1	26.3	204	204	1832	840	3	0:30	Cracked halfway	15:00	2.9	7.7	59
	CS-10	–	1.69	0.1	50.6	203	204	3504	680	6	–	None	15:00	2.4	5.8	54
	CS-12	–	1.69	0.1	50.7	203	204	3496	880	4	1:05	Cracked halfway	15:00	1.8	4.0	60
	CS-14/2	16	–	–	25.4	202	201	–	870	10	–	None	6:50	1.2	~	67
HLM-85	HLM85-1	14	~1.8	0.09	25.7	156	Round	817	730	2	1:25	Shattered	1:30	2.4	1.8	13
	HLM85-2	3,14	~1.8	0.6	~24	156	Round	821	790	1	0:55	Cracked through	1:00	~0.8	0.5	21
G-90	G90-1	14	~1.9	0.09	24.5	155	Round	903	770	2	–	None	15:00	≤0.6	5.3	11
	G90-1/2	11	–	–	23.9	155	Round	855	770	4	–	None	15:00	3.0	15.2	23
	G90-2	7,14,20	~1.9	0.09	25.0	155	Round	874	870	6	–	None	11:10	2.1	≤10.9	16
B-1	GPAN-DL-1	–	0.54	0.03	0.43	190	196	8.73	760	3	0:30	Hole through	0:30	0.43	59.0	62
Silicon Carbide																
Honeycomb	SiC-1	8,14	0.81	0.06	32.0	112	142	313	810	7	0:01	Shattered	1:05	32.0	5.4	34
NC-400 plate	SiC-2	14	2.58	0.1	6.3	95	204	304	760	2	0:01	Shattered	0:01	6.3	9.9	39
Silica																
Slip cast, high purity	SiO₂-JSS-1	13,14	1.95	1.0	18.4	153	204	927	680	1	4:00	Slumped under rods	5:30	5.4	0.5	4
	SiO₂-JSS-1/2	11	–	~	18.4	153	204	922	770	2	1:25	Slumped	1:25	0.3	0.0	18
	SiO₂-JH-1	–	1.92	1.0	20.8	158	158	997	740	4	1:40	Slumped	1:45	0.76	0.10	44
	SiO₂-JH-1/2	11	–	–	20.8	158	158	996	790	3	1:30	Slumped	1:40	0.38	0.0	58
Slip cast, commercial purity	SiO₂-DW-2	–	1.88	0.9	19.5	208	209	1596	840	6	0:09	Dripped	1:00	10.3	1.5	35
	SiO₂-DW-4	14	0.77	0.9	26.5	207	180	532	850	2	0:09	Dripped	0:09	3.1	4.1	43
Fibrous	SiO₂-FRCI-12	6	0.23	0.05	41.0	150	150	210	770	4	0:07	Dripped	0:12	34.9	3.8	28
Silicate																
Mullite, honeycomb, fine	Mul1-1	8,14	0.86	0.1	31.8	140	201	524	860	9	0:04	Melted	0:18	15.6	8.8	31
coarse	Mul1-2	8,14	0.88	0.5	38.0	93	155	330	620	7	0:04	Melted	0:15	6.7	1.5	32
	Mul1-3	9,14	0.88	0.8	38.1	137	172	718	770	7	0:01	Melted	0:05	4.4	0.8	33
Processed kaolin fibrous board	WP-1	–	0.24	0.8	27.1	203	203	265	740	3	0:03	Melted	0:06	27.1	4.9	52
Cordierite honeycomb	CD-MA-1	8	0.46	0.5	25.2	142	Round	185	700	5	0:02	Melted through	0:08	10.0	4.9	45
Alumina-boria-silica cloth	NT-312-5H-26-1	–	0.86	0.8	0.51	78	71	31.8	870	2	0:01	Melted through	0:04	0.51	59.9	47
	NT-312-5H-40-1	–	1.17	0.8	0.68	201	199	35.4	920	4	0:01	Melted through	0:02	0.68	4.4	61

(continued)

Table 2-1. Solar Walk-off Tests: Materials and Test Results (cont'd)

Material and Type	Sample No.	Notes	Bulk Density, g/cm³	Approx. Reflectance	Dimensions Before Test, mm (Note 10)			Mass before Test, g	Insolation during Test, W/m²	Wind Speed during Test, m/s	Fracture or Melting during Test		Duration of Test, min:sec	Lost in Test		Test No.
					Thickness	Approx. Width	Approx. Height				Time, min:sec	Nature		Thickness, mm	Mass, %	
Alumina																
APA-3 paper, 1-ply	Al₂O₃-1A1	–	~0.7	0.9	0.44	202	202	12.3	710	1	0:02	Melted through	0:05	0.4	2.4	10
rigidized	Al₂O₃-1B	18	~0.8	0.9	0.53	202	203	18.0	690	1	0:06	Melted through	0:08	0.5	5.5	12
2-ply	Al₂O₃-2B1	–	~0.9	0.9	0.96	204	205	42.8	760	–	0:02	Melted through	0:05	1.0	5.3	7
3-ply	Al₂O₃-3B	–	~0.9	0.9	1.40	205	205	51.0	790	–	0:05	Melted through	0:06	1.4	35.7	8
Zirconia																
0872, Slip cast and sintered	JSZ-1	14	3.77	0.5	28.6	203	206	3966	710	–	0:17	Melted	0:30	3.0	0.3	6
ZYFB6, Fibrous board	ZYFB6-1	–	0.70	0.9	24.6	204	204	717	650	–	1:00	Melted through	1:35	24.6	0.6	5
ZYW30A, Cloth	ZWY30A-1	17	~1.2	0.9	0.50	204	205	24.3	650	1	0:08	Melted slits	0:12	0.5	2.1	9
Copper																
Electrolytic	Cu-1	3,19	8.87	0.6	25.6	152	155	5351	780	6	2:00	Melted	2:00	2.7	0.8	15
	Cu-1/2	2,11,21	–	0.8	25.4	152	155	5309+	720	2	2:50	Melted	2:55	6.0	0.9	25
	Cu-1/3	5,11	–	0.06	25.4	152	155	5264	690	4	0:50	Melted	0:50	8.9	0.2	27
Aluminum																
T6061	18-17	4	2.70	0.8	1.77	24	Round	–	790	10	0:01	Melted completely	0:04	1.8	–	17
Steel	SS-1	22	~1.39	–	1.98	225	225	139	870	2	0:02	Melted through	0:04	0.99	5.8	47
Polytetrafluoroethylene	PTFE-1	–	2.17	1.0	37.8	203	202	3367	530	5	0:01	Pieces popped off	0:02	4.6	0.3	46
	PTFE-1/2	11	–	–	33.2	203	202	3356	790	4	2:05	Melted	2:10	15.0	9.5	48
	PTFE-1/3	11	–	–	18.2	203	202	3037	730	11	5:50	Melted through	5:50	18.2	41.2	55

NOTES:

1. White coated with boron nitride in aluminum phosphate binder.
2. White painted with 2500 white.
3. White painted with VHT SP-101 flat white.
4. White painted with zinc orthotitanate paint.
5. Black painted with 2500 flat black.
6. Black glazed with borosilicate glass.
7. Tested wet.
8. Tested with sunlight striking open end of honeycomb.
9. Tested with sunlight striking closed side of honeycomb.
10. Thickness listed includes coatings, if any.
11. Test continued on preceding sample. Sample CS-1 was reversed in holder for CS-1/3. Cu-1 was repainted for Cu-1/2 and reversed for Cu-1/3. SiO₂-JSS-1 and SiO₂-JH-1 were reversed for SiO₂-JSS-1/2 and SiO₂-JH-1/2, respectively.
12. Recut from previously tested sample.
13. Not considered a fair test because melting was initiated by hot support rods.
14. Shape irregular.
15. Temperature test. CS-1/3 duration 12:20, interrupted after 7 minutes. CS-1/4 duration 15:00, interrupted after 10 minutes to observe sample. Temperature reached >1150°C (2100°F).
16. Temperature test. Testing continued on sample CS-14 (See Table 2-3). Test plane 50 mm farther from concentrator vertex than in other walk-off tests (Table 3-1). Temperatures reached 1870°C (3400°F).
17. Coating did not cover well; some patches had reflectance of 0.6.
18. Test interrupted after 6 seconds. Test resumed after sample was observed.
19. Test interrupted after 1 minute. Test resumed after sample was observed.
20. Support rods oxidized through; let sample fall; terminating test.
21. Melting may have been initiated by hot support rod.
22. SS-1 mounted behind NT-312-5H-26-1 during test.

Table 2-2. Solar Acquisition Tests: Samples and Results

Material: Graphite Type CS

Sample No.	Notes	Bulk Density, g/cm^3	Approx. Reflectance	Dimensions Before Test, mm			Mass Before Test, g	Insolation During Test, W/m^2	Wind Speed During Test, m/s	Cycle, s		No. of Cycles	Duration of Test, min	Lost in Test		Test No.
				Thickness	Approx. Width	Approx. Height				On	Off			Thickness, mm	Mass, g	
CS-5	1	1.76	0.1	36.7	207	207	2756	955	2	1.1	9.2	699	113	7.0	4.7	J-41
CS-7	-	1.69	0.1	26.3	204	204	1886	780	5	0.9	10.1	1000	183	2.2	2.0	53
CS-7/2	2	-	-	24.1	204	204	1849	930	10	0.9	10.1	1000	183	2.4	0.7	57

Notes:

1. For first 15 cycles, off time = 19.2 seconds.

2. Test continued on preceding sample.

Table 2-3. Solar Spillage Tests: Samples and Results

Material: Graphite Type CS. Bulk Density: 1.69 g/cm^3. Approximate Reflectance: 0.1.
Edge closest to solar spot was tapered (Figure 2-1).

Sample No.	Notes	Dimensions Before Test, mm			Axial Distance From Concentrator Vertex, m (Note 1)	Radial Offset of Solar Spot, mm	Distance From Spot Center to Nearest Edge of Sample, mm	Solar Concentration at Edge	Insolation During Test, W/m^2	Flux Density at Sample Edge, kW/m^2	Flux Density as % of Peak Flux Density at This Axial Distance	Wind Speed During Test, m/s	Duration of Test, min:sec	Temperature Reached, °C	Lost in Test, Width or Height, mm	Test No.
		Thickness	Approx. Width	Approx. Height												
CS-13	2	26.5	197	203	6.556	100	175	15	830	10	0.18	3	19:40	107	0.0	J-63
CS-13/3	3	26.5	197	203	6.492	0	125	40	890	40	0.25	2	25:00	133	0.0	65
CS-13/2	3	26.5	197	203	6.492	0	100	80	850	70	0.5	1	26:30	173	0.0	64
CS-13/4	3	26.5	197	203	6.492	0	75	450	890	400	3.	6	15:10	312	0.0	66
CS-11/3	4,5	26.1	203	50	6.553	54	100	600	850	500	7.	13	10:50	702	0.0	56
CS-11	6	26.1	203	76	6.537	54	75	1500	870	1300	15.	7	5:20	(640)	0.0	50
CS-11/2	3,5	26.1	203	76	6.537	54	75	1500	650	1000	11.	4	13:00	798	0.0	51
CS-14	2,7	25.4	202	201	6.492	100	70	700	830	600	5.	3	19:40	-	1.6	63

Notes:

1. For comparison of pertinent axial distances, see Table 3-1.
2. Nearest edge of specimen was offset from axis in direction radially opposite to solar spot.
3. Testing continued on sample which had next lower digit after slash.
4. Sample recut from CS-11/2.
5. Nearest edge of specimen was offset from axis in direction 135° from solar spot.
6. Temperature had not reached constant value at end of test.
7. Sample edge not tapered.

0.20

0.129 DRILL

1.0

SUNLIGHT 0.25 R 45°

0.20

DIMENSION A: 2.0, 3.0, 7.8

A

2.0

2 THERMOCOUPLE HOLES
THERMOCOUPLES #30 GAGE
CHROMEL - ALUMEL
IN 0.125 D DOUBLEBORE
CERAMIC INSULATOR

8.0

2.0

SPILLAGE TEST SAMPLE
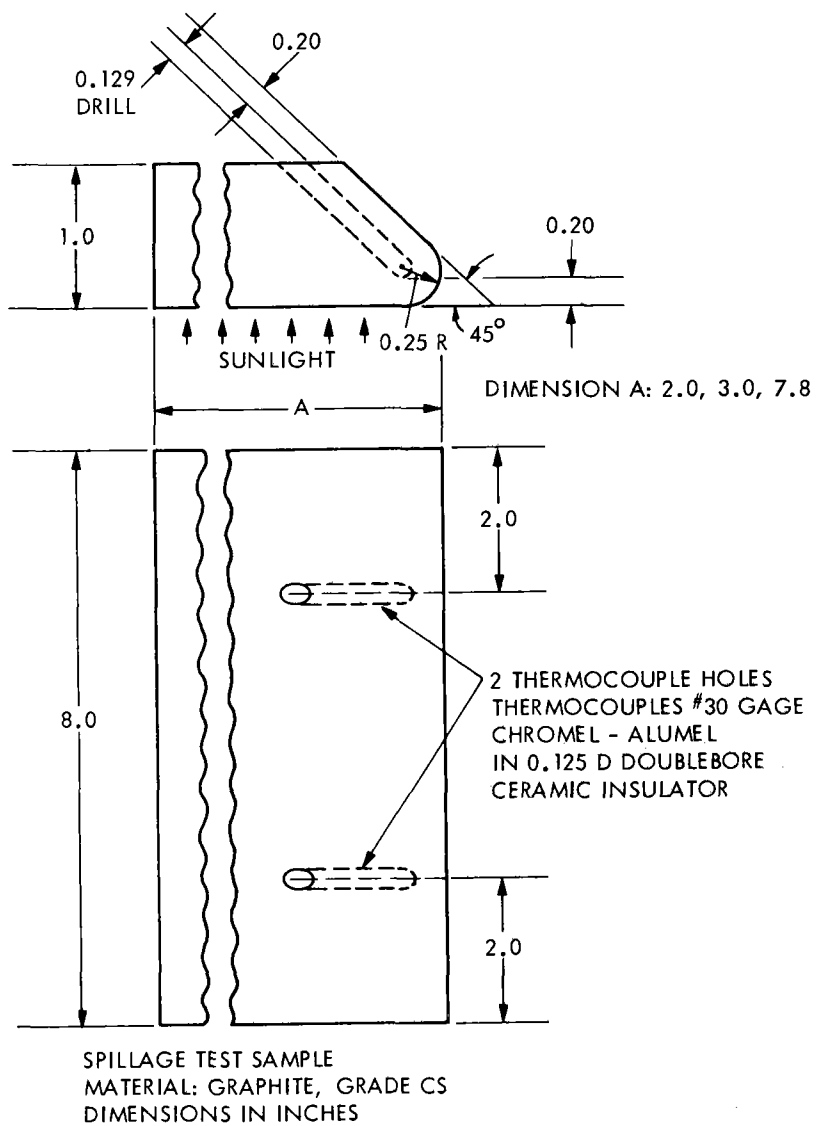MATERIAL: GRAPHITE, GRADE CS
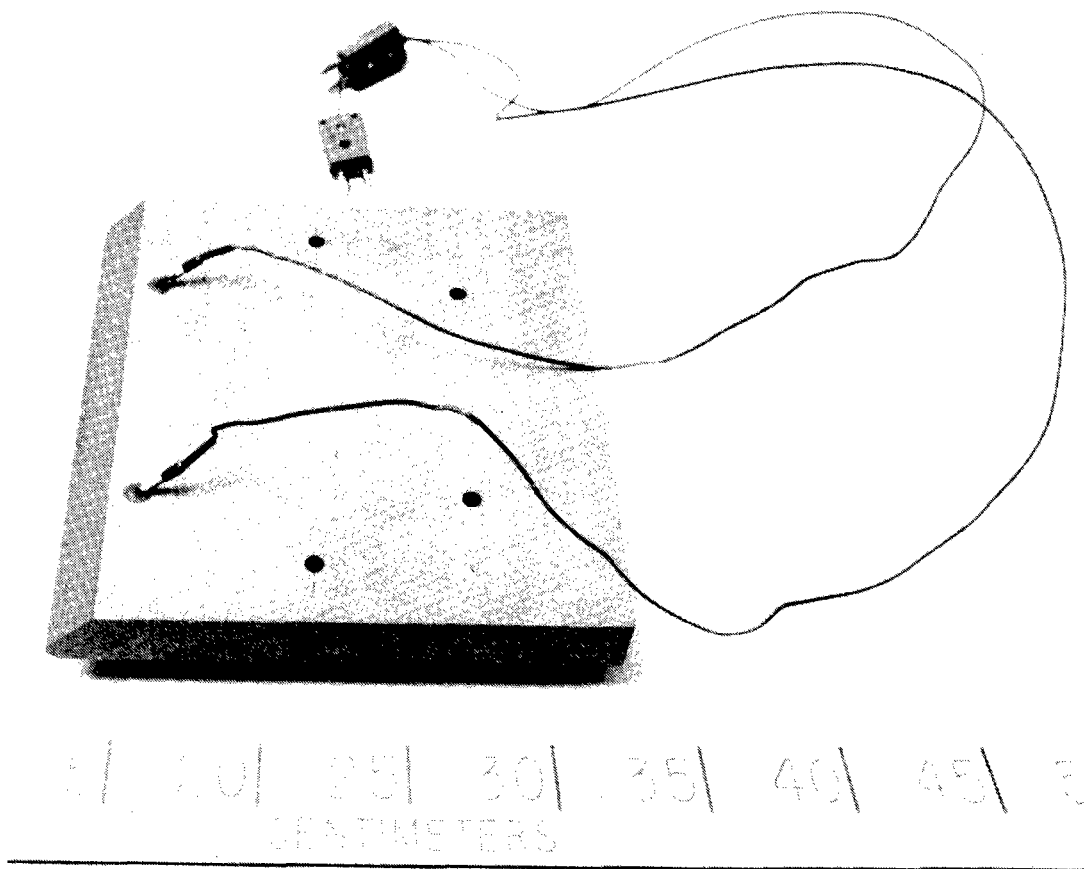DIMENSIONS IN INCHES

Figure 2-1.   Sample for Spillage Test

Figure 2-2. Spillage Test Sample, Exposed.
(Side Away from Concentrated
Sunlight.   Sample CS-13/4.)

SECTION III

TEST EQUIPMENT

Solar tests were made on Test Bed Concentrator 1 (References 12 through 16) at the Jet Propulsion Laboratory's Parabolic Dish Test Site, Edwards, California. This concentrator utilizes 220 spherical mirrors to gather the sunlight. Each mirror can be individually adjusted, so the flux pattern in the focal region can be tailored to the needs of the test being conducted. In this report, positions on the concentrator are referenced to its optical axis and its vertex (the point where the axis intercepts the reference paraboloid of the mirror surfaces).

As part of the setup for testing a major portion of the FACC organic Rankine module (receiver plus engine/generator, rectifier, and control units), a water-cooled aluminum shield had been mounted near the focal plane of the concentrator. This shield has a central opening 400 mm (16 in.) in diameter. A water-cooled aluminum sliding shutter, installed on the side of the shield closest to the concentrator mirrors, can be opened or closed to permit concentrated sunlight to pass through the shield opening or to block it off.

A.   SOLAR WALK-OFF AND SOLAR ACQUISITION

For the materials walk-off and acquisition tests, a fixture was designed which mounted against the aluminum shield, on the side away from the mirrors (Figures 3-1 through 3-3). The test fixture was in the form of a "window-frame" with outside dimensions of 380 x 330 mm (15 x 13 in.), and an opening 230 mm (9 in.) square. The sample was placed in this opening. The fixture was 114-mm (4-1/2-in.) thick and made from graphite, grade 3499. (See Appendix A for details of this grade.) A key aim of the fixture design was to minimize conductive heat transfer from sample to test fixture and from test fixture to water-cooled shield. This was done primarily to reduce thermal gradients in the fixture and thus reduce the likelihood of its fracturing because of thermal shock. The surface of the fixture that bears against the water-cooled shield was cut in two directions with grooves (Figure 3-4), so the contact area for heat transfer between fixture and shield was small. The fixture was mounted to the shield by four steel studs inserted into tapped holes in the square aluminum section which bounds the aperture of the shield. A tubular alumina insulator surrounded each stud to reduce heat transfer from fixture to stud, and a flat alumina insulator was used under the steel washer and nut that secured the fixture on each stud. The sample was retained by rods 10 mm (3/8 in.) in diameter, made of graphite, grade 580, 873S, or HC (see Appendix A). Rods were used to minimize thermal contact between support and sample. To reduce thermal contact between rods and fixture, the rods fitted loosely through 12-mm (1/2-in.) holes in the upper frame of the fixture and rested in blind holes, of the same diameter, in the lower frame. To accommodate samples of various sizes and thickness, multiple rows of holes were drilled for the rods (Figures 3-1 and 3-4). The row of holes and rods closest to the mirrors served to define the position of the sample relative to the concentrator focus; during testing, when the concentrator was elevated to
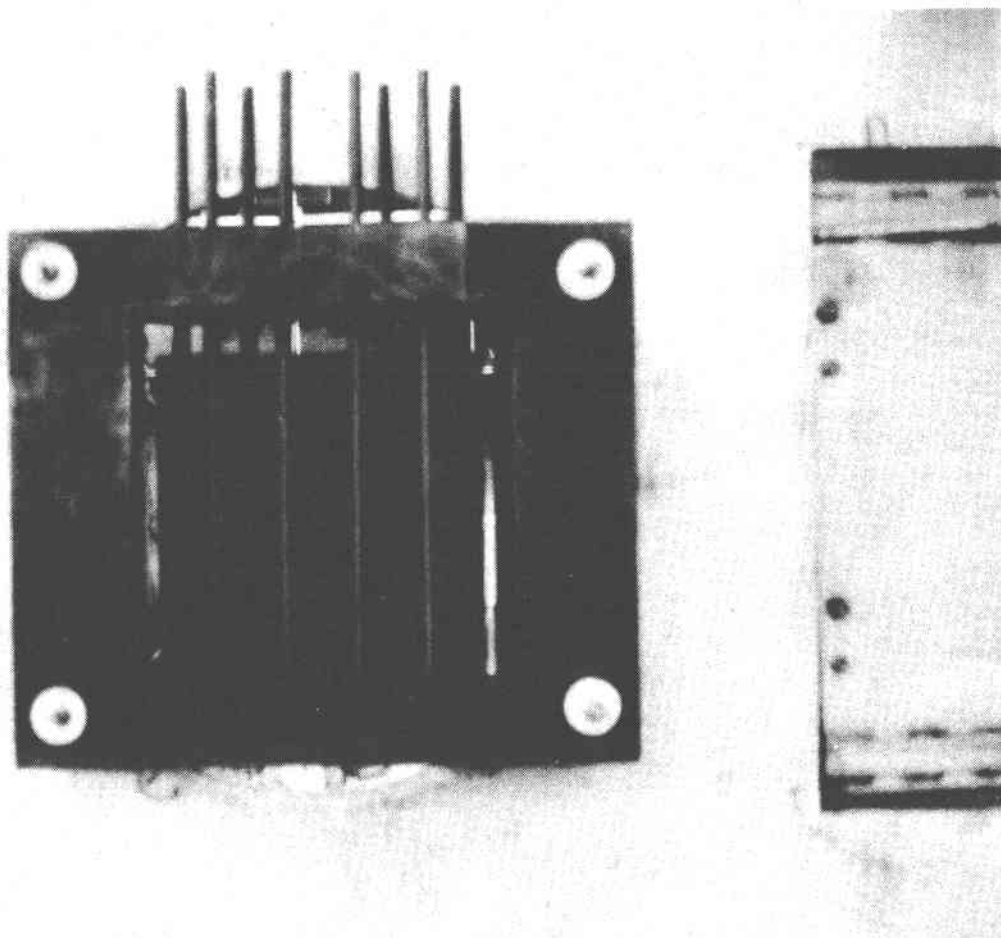
Figure 3-1.   Test Fixture Drawing

Figure 3-2. Test Fixture on Concentrator. View Looking Toward Mirrors

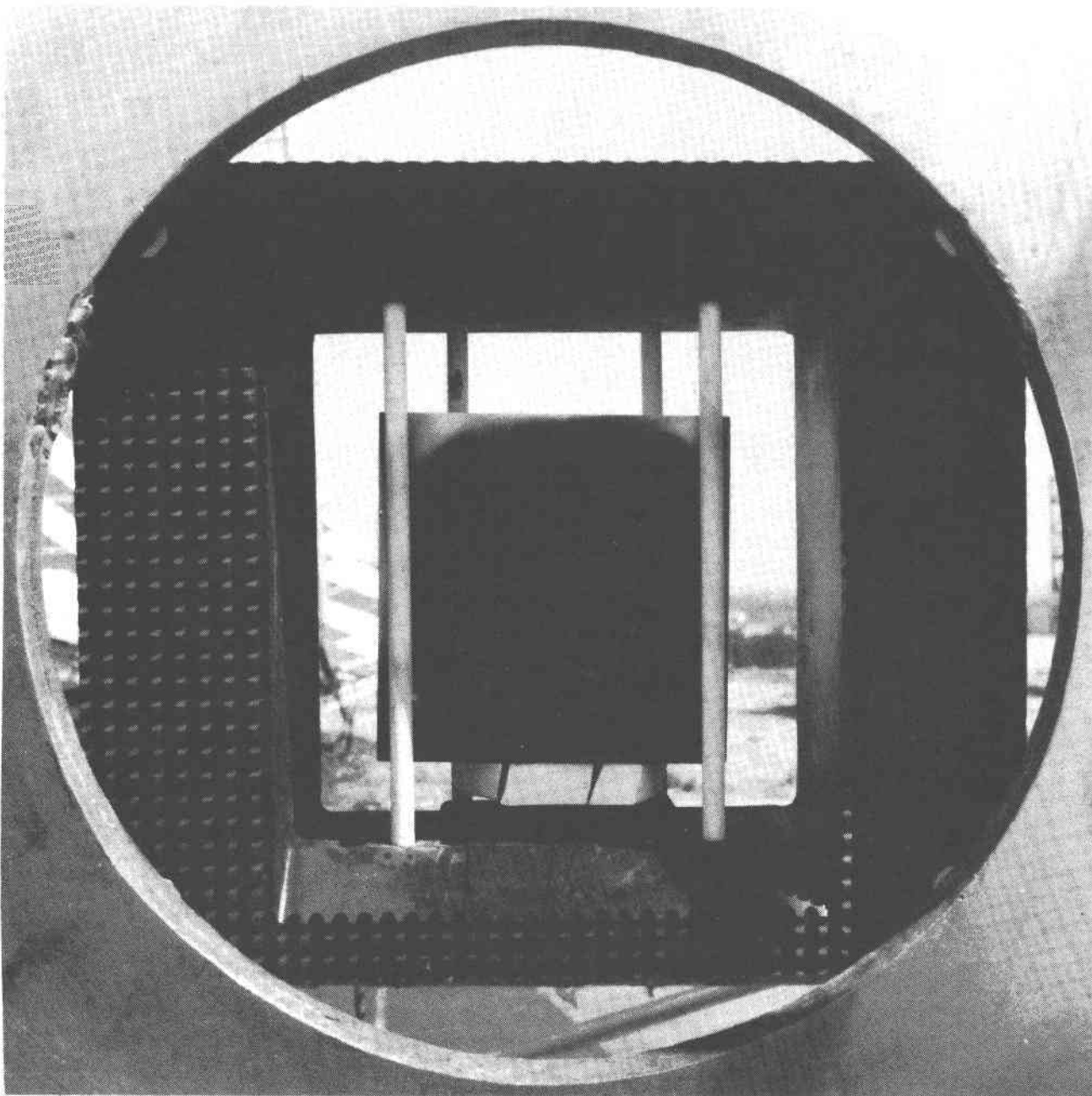Figure 3-3. Test Fixture on Concentrator. View Looking Away from Mirrors. [Fibrous silica sample (SiO_2 – FRCI-12) mounted in fixture. Photographed after sample was tested.]
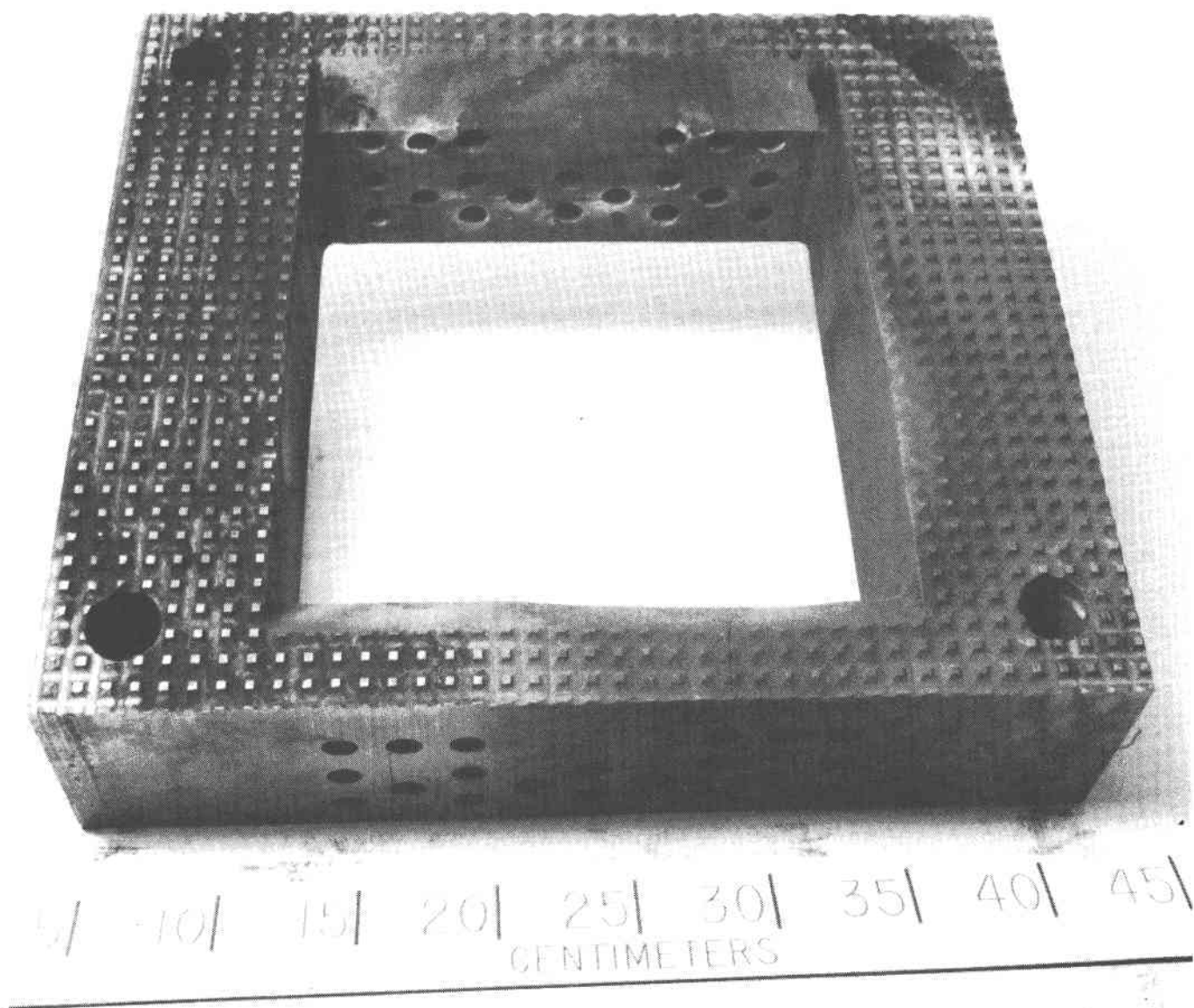
Figure 3-4. Test Fixture After 61 Tests

point at the sun, gravity kept the sample flat against these rods. The top and bottom edges of the fixture aperture adjacent to these rods were chamfered to reduce blockage of concentrated sunlight by the fixture. The support rods caused some blockage, which somewhat increased the thermal gradients and thermal stresses in the samples. When heated, the sample, support rods, and test fixture could each expand thermally with little restraint, which minimized externally applied stresses. During exposure, the center of the solar spot was close to the center of one face of the sample.

For tests of major elements of the organic Rankine module, the pointing of individual mirrors on the test bed concentrator and the position of the receiver aperture were set, as listed in Table 4, to simulate the corresponding distribution of concentrated sunlight expected with Parabolic Dish Concentrator 1 (PDC-1), the concentrator then planned for use with the FACC organic Rankine module. The receiver was designed for a flux pattern peaking at 7000 kW/m^2 in the aperture plane at an insolation of 1 kW/m^2. During walk-off and solar acquisition testing, the side of the sample facing the mirrors was positioned about 25 mm (1 in.) closer to the mirrors (and to the focal and aiming planes) than the position of the receiver aperture during module test (Table 3-1). The distribution of solar flux in this test plane was measured with a flux-mapper (References 17,18) and is shown in Figure 3-5, normalized to an insolation of 1 kW/m^2. Figure 3-5 shows peak measured flux density in the materials test plane of 9700 kW/m^2 at an insolation of 1 kW/m^2. In the walk-off tests, the actual insolation was lower than 1 kW/m^2; at an insolation of 720 W/m^2, the peak flux density was 7000 kW/m^2. Figure 3-5 shows that the flux density (at 1 kW/m^2 insolation) fell to 2600 kW/m^2 at a diameter of 10 cm (4 in.) centered around the peak, and to less than 1 kW/m^2 at a diameter of 380 mm (15 in.), the design diameter of the receiver aperture. The total concentrated solar power at 1 kW/m^2 was approximately 78 kW, as measured by a cold-water calorimeter (Reference 19).

B.   SOLAR SPILLAGE

For spillage tests, the test samples were mounted at various radial and axial positions to simulate spillage conditions that might be encountered with the organic Rankine and with other solar thermal power modules (Tables 2-3 and 3-1). For some of these tests, the spillage sample was mounted in the text fixture used for walk-off tests, but off center so that only the edge of the solar spot struck the sample. [This required use of a spillage sample with height limited to 50-75 mm (2-3 in.).] In other spillage tests, the test fixture was removed and the axial position of the water-cooled shield was adjusted. A bracket was fastened to the shield and the sample bolted to the bracket (Figures 3-6, 3-7). A spacer kept the sample from touching the cold shield. Also with this arrangement, only the edge of the solar spot struck the sample.

Table 3-1. Axial Positions on Test Bed Concentrator 1

| Item	Distance From Concentrator Vertex, m	in.
Test plane, samples CS-13/2, -13/3, -13/4, -14	6.492	255.6
Alignment point, middle and outer (B & C) mirrors	6.493	255.6
Alignment point, inner (A) mirrors of concentrator	6.525	256.9
Test plane, walk-off and acquisition tests (also CS-11, -11/2)	6.537	257.4
Test plane, sample CS-11/3	6.553	258.0
Test plane, sample CS-13	6.556	258.1
Aperture plane, organic Rankine receiver	6.563	258.4
Test plane, sample CS-14/2	6.588	259.4
Mounting plane, receiver	7.220	284.2
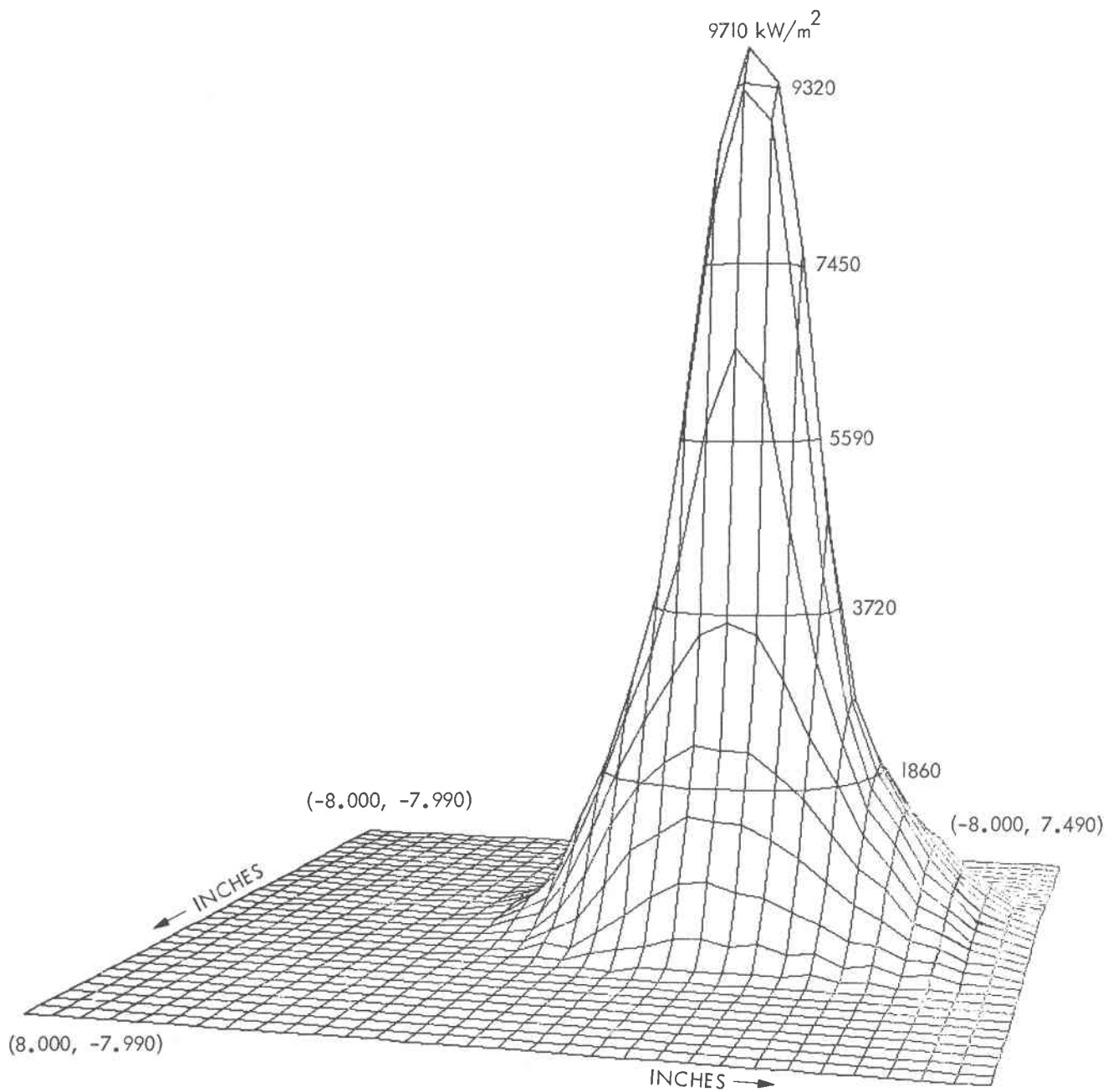
Figure 3-5. Flux Map in Plane of Walk-off Testing.
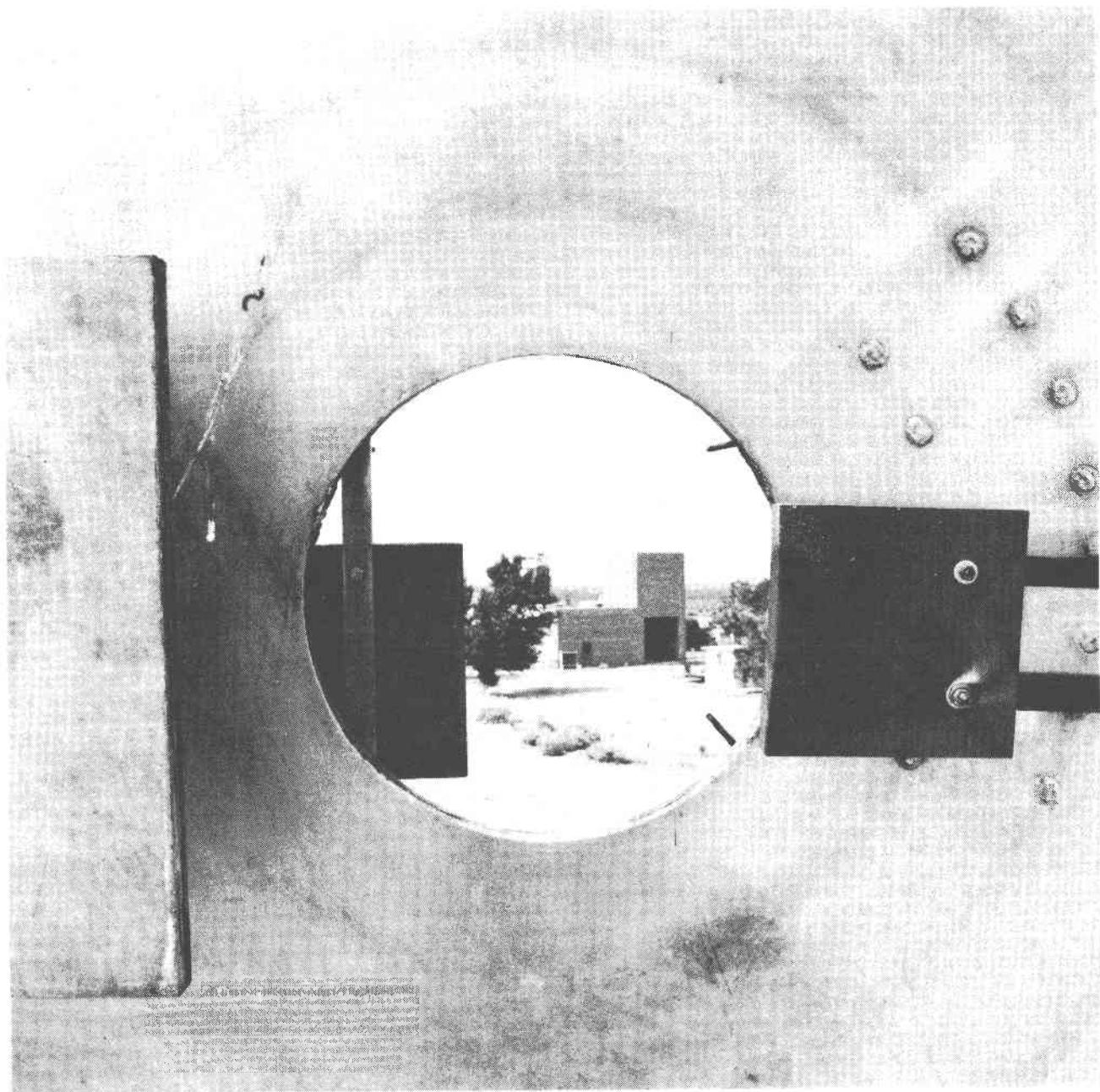(After Owen, Reference 18)

Figure 3-6. Spillage Test Setup for Graphite Sample CS-13.
View Looking Away From Mirrors. (CS-13 at
left. CS-14 installed at right to protect
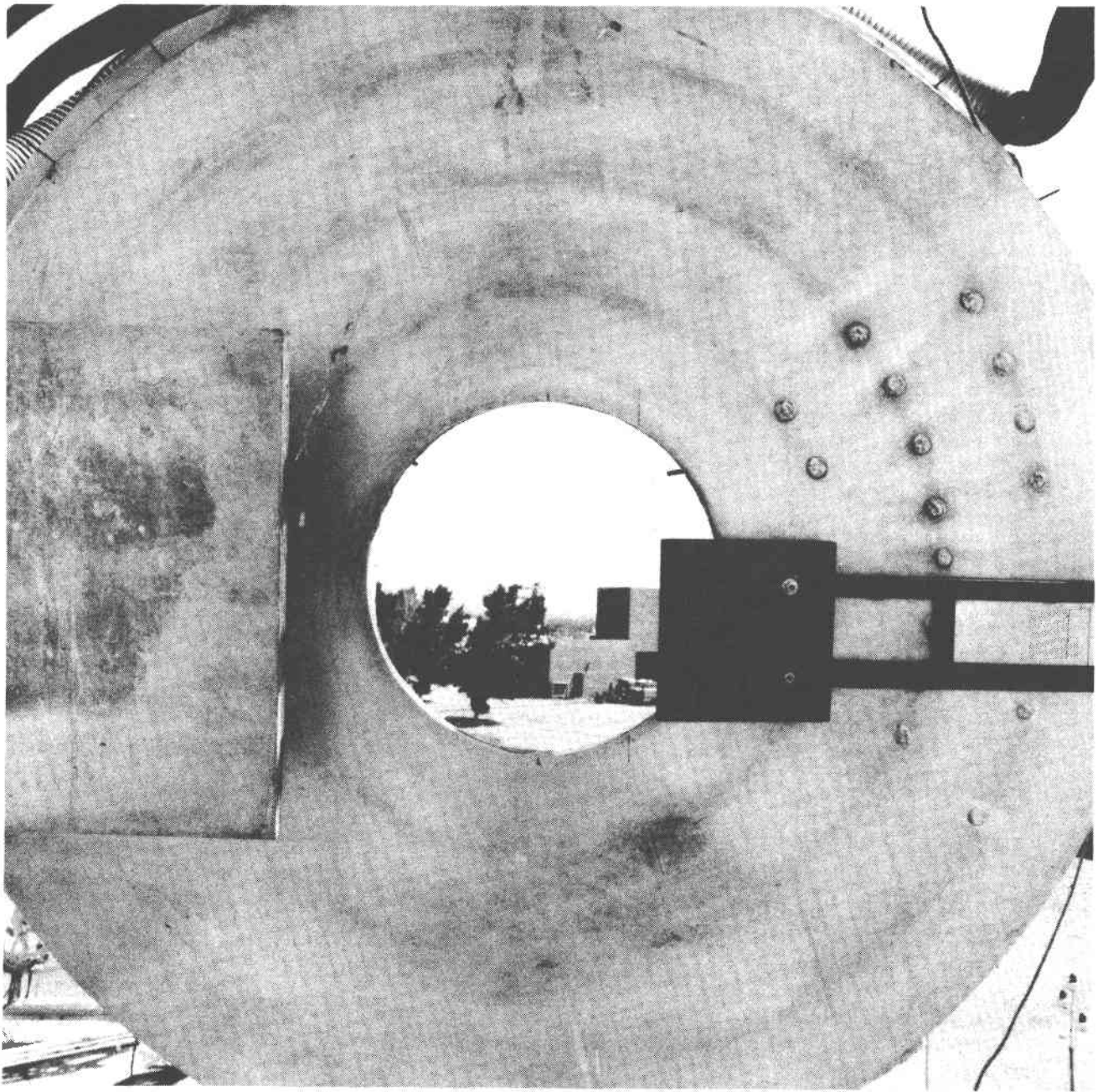water-cooled shield from concentrated sunlight.)

3-9

Figure 3-7. Spillage Test Setup for Graphite Sample CS-13/4.
View Looking Away From Mirrors. (Shutter, open,
is at left.)

SECTION IV

TEST PROCEDURES

A.   SOLAR TESTS, GENERAL

A lower insolation threshold of 600 W/m^2 was chosen for the tests.
Measured direct normal insolation during tests was 530 to 960 W/m^2.

In all solar tests, samples were observed on television utilizing a
black-and-white TV camera mounted on a receiver support leg of the concen-
trator. The operator could control the iris, focus, and focal length (zoom)
of the camera from his station. Because of the limited dynamic range of the
TV system, the wide variations in brightness encountered when going on sun,
and the varying reflectivity of the samples, about 10 seconds were usually
needed to adjust the TV to give a satisfactory image of the sample; thus,
useful TV observations generally started about 10 seconds after the shutter
was opened.

The television imagery was recorded on a video cassette recorder.
Insolation was recorded digitally, at 20-second intervals, using Eppley
pyroheliometers on the concentrator and on the ground nearby and a Kendall
pyroheliometer on the ground. Weather data, including wind velocity and
additional insolation data, were recorded digitally at longer intervals.

The concentrator mirrors were washed immediately prior to the start of
the materials solar testing program and twice during the series of materials
tests. They were also cleaned by rain at various times during the testing
period.

B.   SOLAR TESTS, WALK-OFF

Primary emphasis in the test program was devoted to walk-off; all of the
types of materials investigated were tested for their ability to sustain walk-
off.

Each sample was mounted in the test fixture and graphite rods inserted
to retain it. After initial experience, two rods were placed on the
illuminated side of each sample (the side toward the mirrors), spaced as far
apart as sample dimensions permitted, except for samples that were unusually
heavy or expected to survive a long time. For these, four rods were used on
the illuminated side. Additional rods were used on the back of the sample
(side away from the mirrors).

When the insolation was above threshold, the concentrator was pointed at
the sun, with the shutter closed, and set to track the sun automatically. The
shutter was then opened and the sample observed in three ways:

(1)   An observer using dark glasses and binoculars was stationed in the
      shadow of the concentrator and watched the sample throughout each
      test through an opening in the center of the mirror array.

(2)   The concentrator operator watched the sample on television.

(3)   Both individuals listened for sounds from the sample, the observer directly by ear and the concentrator operator via a microphone mounted near the sample.

Tests of ability to withstand walk-off were terminated by closing the shutter 15 minutes after it was opened, or when the sample failed, whichever occurred first. For this purpose, failure was initially defined as visual observation of cracking, melting or dripping, or aural observation of loud noise from the sample (noise was generally due to shattering). (To reduce the risk of damage to the concentrator mirrors from falling fragments or hot drops, tests were generally constrained to sun elevations below 45 degrees.) It was found during testing that some samples cracked partway, but did not fall apart; the procedure was later changed to continue the test despite such cracking. Also, some samples that survived the test without melting or cracking apart were retested for total exposure times up to 45 minutes.

Several samples were tested wet to simulate exposure to rain followed by sunlight and walk-off. They were soaked in water at a depth of 15 to 30 cm (6 to 12 in.) for at least 30 minutes prior to solar testing.

Temperature estimates during walk-off tests were obtained for two graphite samples by observing the samples with an infrared pyrometer and by eye (i.e., noting the color of the emitted light) after the shutter was closed and the concentrator swung off sun. Another graphite sample was observed with the infrared pyrometer during exposure after the insensitivity of the pyrometer to reflected sunlight had been confirmed. Also, one sample of aluminum was supplied with a thermocouple attached. Because of the small size of this sample (24 mm in diameter and 1.8 mm thick), a special adapter was used to mount the sample, with the thermocouple, in the test fixture (Figure 4-1). The temperature of this sample was recorded with a strip-chart recorder.

C.   SOLAR TESTS, ACQUISITION

Tests aimed at evaluating behavior under acquisition/deacquisition and spillage conditions were conducted on only one type of material: graphite. These tests were run because some grades of graphite appeared promising in the walk-off tests and because of concern that the rate of loss of graphite by oxidation might be excessive under the long cumulative exposures associated with acquisition/deacquisition and spillage.

Two graphite samples were tested under conditions simulating repeated acquisition and deacquisition. They were mounted in the same way as the samples for walk-off testing. The acquisition/deacquisition tests consisted of multiple cycles of opening and closing the shutter, each approximately 1 second open, 10 to 19 seconds closed. Maximum exposure was 2000 cycles.
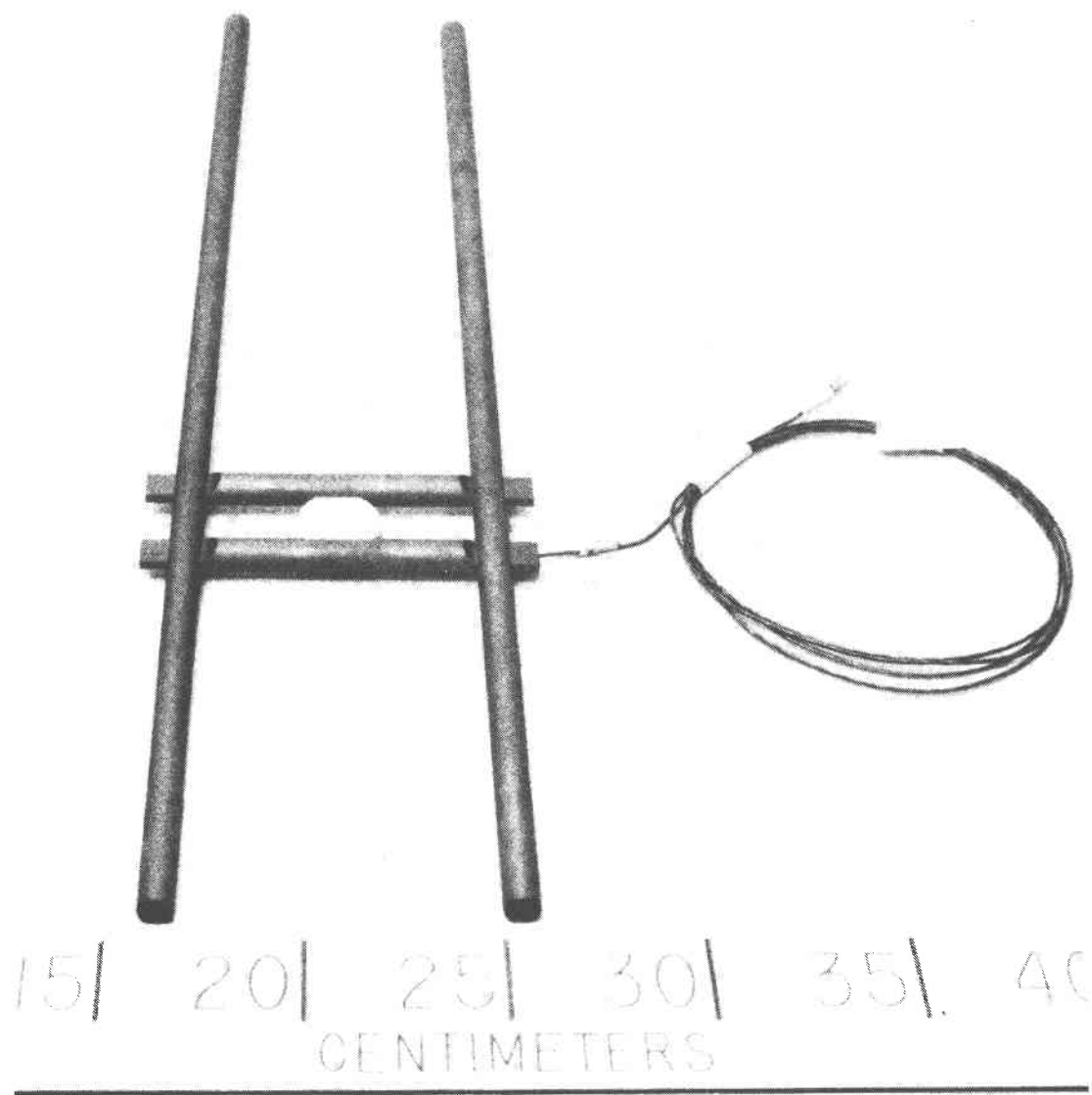
Figure 4-1. Aluminum Sample (18-17) in Adapter, with Attached Thermocouple

D.   SOLAR TESTS, SPILLAGE

Solar tests of the extent of oxidation of graphite under conditions simu-
lating many thousand hours of spillage exposure were beyond the scope of this
work. Instead, measurements were made of the lip temperature of graphite
samples simulating a tapered aperture lip (Figures 2-1 and 2-2). Thermo-
couples were inserted within the lip, which was placed, during exposure, 75 to
175 mm (3 to 7 in.) from the center of the spot of sunlight [representing
aperture diameters of 150 to 350 mm (6 to 14 in.)] and at various axial
positions (Tables 2-3 and 3-1). Exposure was initiated by acquiring the sun
with the concentrator or by opening the shutter. Flux density at the lip
position nearest the spot center (which was also a thermocouple position)
varied from less than 1 to over 1000 kW/m^2 at the measured insolation
(Table 2-3); the rest of the sample was at lower flux density. Thermocouple
readings in these tests were recorded digitally, at 20-second intervals. The
test was generally terminated when thermocouple readings became constant.

E.   MEASUREMENTS BEFORE AND AFTER SOLAR TEST

All samples were weighed, measured, and observed visually before and
after solar testing. They were photographed in color after, and usually
before, each solar test. Bulk densities prior to testing were calculated from
the measured dimensions and weights. For samples of irregular shape, areas
for this calculation were determined by tracing the sample outline on paper,
cutting out the tracing, and weighing it.

To provide a rough measure of solar absorptance at minimum cost, sample
brightness was measured outdoors, in open shade, with a Pentax-type brightness
meter designed for use in photography, and compared with the brightness of
Kodak white and gray reflectance standards placed adjacent to the sample.
These standards are stated to have reflectances of 90 and 18%, respectively.
Viewing with the brightness meter was at an angle of about 45 degrees to the
sample surface. An approximate solar reflectance was calculated from the
brightness data by the relation:

$$\frac{\text{Reflectance of Sample}}{\text{Reflectance of Standard}} = \frac{\text{Brightness of Sample}}{\text{Brightness of Standard}} \tag{1}$$

SECTION V

WALK-OFF TESTS: MELTING AND FRACTURE RESULTS

Results of the walk-off tests and accompanying measurements are tabulated in Table 2-1 and summarized in Table 5-1. Photographs of all samples after test are shown in Appendix B. The great majority of the samples tested under simulated walk-off conditions melted, shattered or fractured, many of them within the first few seconds of solar exposure. The only materials tested that appeared promising for walk-off protection were graphite grades G-90 and CS, graphite cloth, and high-purity slip-cast silica. (See Appendix A for characteristics of the materials used.)

A.   GRAPHITES

1.   Grade G-90

Graphite, grade G-90, was the only material that consistently survived a 15-minute simulated walk-off without melting, slumping, or cracking. A sample of G-90 survived two successive 15-minute tests without cracking (Figures B-29 and B-30). (Graphite cannot be melted at atmospheric pressure.) Another sample of this material was tested wet, and it too did not crack (Figure B-31).

Grade G-90 is an extruded material that is reimpregnated several times with coal-tar pitch and regraphitized to reduce its porosity and increase its bulk density. This grade is used to make throats for solid-propellant rocket nozzles. Grade G-90 is a premium grade and somewhat expensive for a graphite: about $45/kg ($20/lb). A typical aperture plate made of such graphite for the FACC organic Rankine module might be 25 mm (1 in.) thick, 380 mm (15 in.) inner diameter (ID), 760 mm (30 in.) outer diameter (OD), with a mass of about 16 kg (weight 35 lb). The cost of about $700 for the material might be acceptable, but is probably higher than desirable for quantity use.

2.   Grade CS

During the standard walk-off test, all six samples of uncoated graphite grade CS, 14 to 37 mm (0.5 to 1.5 in. thick), developed a single crack extending from near the midpoint of an edge to near the center of the specimen (Figures B-5, B-7, B-11, and B-13). This reproducibility was striking, particularly because the samples came from three different lots of graphite. Of two samples that were 50 mm (2 in.) thick, one survived the simulated walk-off test without cracking or other failure; the other cracked somewhat more than halfway. In some of the grade CS samples, the crack was observed to advance gradually from edge to center. Only in the 50-mm-thick sample did the crack advance any further. None of the CS graphite specimens fell apart into two or more pieces. Two samples of CS graphite that cracked halfway during initial exposure were retested for a total of 17 minutes and (with occasional interruptions) 45 minutes, respectively, without further

Table 5-1. Summary of Results of Walk-off Tests

Material Type		Thickness, mm	Failure Mode	Time
Graphite	3499	26	Shattered	1 to 8 min
	8826	26	Shattered	1 to 1-1/2 min
	CS	14-50	Cracked halfway (1 of 10 survived)	10 s to 14 min
	HLM-85	24-26	Shattered	1 to 1-1/2 min
	G-90	24-25	(Survived)	30 min
	Cloth	0.4	Holed	30 s
SiC		6-32	Shattered	1 s
SiO$_2$	Slipcast, high purity	18-21	Slumped	1-1/2 to 4 min
	Slipcast, commercial	20-26	Dripped	10 s
	Fibrous, glazed	41	Dripped	7 s
Silicates	Mullite	32-38	Melted	1 to 4 s
	Processed kaolin	27	Melted	3 s
	Cordierite	25	Melted	2 s
	Alumina-boria-silica	0.5-0.7	Melted	1 s
Al$_2$O$_3$	Paper	0.4-1.4	Melted	2 to 6 s
ZrO$_2$	Cast and sintered	29	Melted	20 s
	Fibrous board	25	Melted	1 min
	Cloth	0.5	Melted	8 s
Copper		26	Melted	1 to 3 min
Aluminum		1.8	Melted	1 s
Steel		2	Melted	2 s
Polytetrafluoroethylene		38	Melted	2 min

observed crack advance (Figures B-6, B-8, and B-9). With two other samples of this grade (one tested wet, one dry), the test was continued to 15 minutes despite the single crack that formed (Figures B-11 and B-13). After the usual post-test examination, these samples were retested another 15 minutes. No further advance of the crack was noted (Figures B-12 and B-14). Apparently the first crack, halfway across, was sufficient to relieve the thermal stresses and prevent further cracking. This suggests that with proper design, including segmenting, CS graphite should provide satisfactory walk-off protection. Bank and Owen (Reference 8) reached a similar conclusion on the basis of earlier tests.

Grade CS is a commercial grade of extruded graphite and has medium grain size and bulk density. It costs about $4.50/kg ($2/lb); an aperture plate of the dimensions mentioned would cost about $65 for the material. (CS would weigh slightly less than G-90 because it is less dense.)

Within the limited range of thickness tested (14 to 50 mm, 0.5 to 2.0 in.), thickness had no obvious effect upon performance of grade CS graphite, except that the thickest samples were less consistent (Table 2-1). This suggests that an aperture plate of this material should be thin to save weight and cost, provided it has adequate resistance to acquisition/ deacquisition and to spillage.

Rough measurements on two samples of grade CS, 25 to 37 mm (1.0 to 1.4 in.) thick, indicated that the temperature reached during 15-minute exposures was above $1870^{\circ}C$ ($3400^{\circ}F$) at a peak flux density of 3300 kW/m^2. At 7000 kW/m^2, the corresponding temperature would be above $2310^{\circ}C$ ($4200^{\circ}F$). This is only a lower limit; as noted below, zirconia, with a melting point of $2600^{\circ}C$ ($4700^{\circ}F$) and a much lower solar absorptance than graphite, melted rapidly during walk-off tests.

Like most graphites fabricated by extrusion, grade CS has markedly anisotropic properties, with its coefficient of thermal expansion being lower and its strength higher in the direction parallel to the grain (parallel to the extrusion direction) than in the direction perpendicular to the grain (perpendicular to the extrusion direction) (Table 5-2). For samples CS-7 through CS-12, and probably for all CS samples, the grain was parallel to one side of the sample. It is very likely that cracking occurred perpendicular to the grain. This directionality should be taken into account in the design of aperture plates made of graphite, and should be controlled during their fabrication.

3.   Effect of Water

Graphite grades G-90 and CS absorbed very little water on immersion, and their subsequent performance in simulated walk-off tests appeared unaffected by this wetting (Table 5-3). Presumably rain would not impair their subsequent value for walk-off protection.

Table 5-2. Nominal Characteristics of Conventional Grades of
Graphites Tested or Used in Test Equipment[a]

Grade	Maximum Particle Size of Binder, μm	Fabrication Method[b]	Bulk Density, Mg/m^3	Thermal Conductivity,[c] W/m°C	Electrical Conductivity,[c] kS/m	Coefficient of Thermal Expansion,[c] 10^{-6}/°C	Flexural Strength,[c] MPa	Approx. Cost, $/kg
580[d]	200	Extruded	1.76	60/–	100/–	1.2/–	29/–	20
3499	75	Molded	1.71	100/–	70/–	2.1/2.8	24/21	13
8826	75	Molded	1.78	–/–	110/–	2.0/2.7	30/25	17
873S[d]	800	Extruded	1.74	180/–	120/–	1.4/2.5	19/–	9[d]
CS	750	Extruded	1.67	160/100	120/80	1.2/2.7	19/13	4
G-90	800	Extruded	1.91	170/120	130/90	1.6/2.2	29/20	50
HC[d]	200	Extruded	1.62	–/–	110/–	–/–	24/–	22[d]
HLM-85	750	Extruded	1.80	–/–	170/–	–/–	21/–	4

Notes:

(a) Values are for room temperature and for size used; from manufacturers' literature.

(b) Raw materials: filler, petroleum coke; binder, coal tar pitch.

(c) Value before slash is for direction parallel to grain (parallel to extrusion direction; perpendicular to direction of pressing in molding). Value after slash is for direction perpendicular to grain. Direction parallel to grain was parallel to thickness direction of sample or test fixture, except for samples CS-7 to CS-12, for which it was in plane of sample. For support rods, direction parallel to grain was parallel to their length.

(d) Grades 580, 873S, and HC were used only as support rods; diameter 10 mm (3/8 in.). Cost and other characteristics are for this size.

Table 5-3. Effect of Water on Subsequent Performance of
Graphites in Walk-off Tests

Wet or Dry	Graphite Type	Graphite Thickness, mm	Sample Number	Insola-tion, W/m^2	Fracture During Test Time, Min:Sec	Nature
Wet	CS	36.7	CS-4	800	2:40	Cracked Halfway
Dry	CS	37.2	CS-3	680	14:00	Cracked Halfway
Wet	G90	25.0	G90-2	870	–	None
Dry	G90	24.5	G90-1	770	–	None

4.   Other Grades of Conventional Graphite

Other grades of conventional graphite tested were 3499, 8826, and HLM-85. All samples of these grades cracked apart or shattered in test; the 3499 at exposure times of 1-1/2 to 8 minutes, the 8826 and HLM-85 in 1 to 1-1/2 minutes (Figures B-1 through B-4, B-27, and B-28). The first two are fine-grained molded grades, the last a medium-grain extruded grade that is reimpregnated and regraphitized.

The test fixture used was of grade 3499 graphite and survived 50 tests without cracking, for a total exposure time of 6 hours. In these tests, the solar spot was centered in the fixture, 115 mm (4.5 in.) from each side, except for the last five minutes when it was intentionally offset, bringing the spot center within 75 mm (3 in.) of one side and the top of the fixture "window frame." In test 51, with another 13 minutes of such offset exposure, the fixture cracked through a top row of drill holes, but remained serviceable through the completion of the program (63 tests with the fixture, 13 hours of solar exposure, including one-half hour with spot offset). (See Figure 3-4.)

None of the 10-mm (3/8-in.) diameter support rods of 580, 873S, or HC grades graphite were observed to fracture in service.

5.   Comparison of Conventional Graphite Grades

Some nominal characteristics of the various grades of conventional graphite are compared in Table 5-2. Grades G-90 and CS, which performed well, are extruded grades with medium grain size (maximum particle size nominally 750 micrometers). Grades 3499 and 8826 are fine-grained molded grades (maximum particle size nominally 75 micrometers); they shattered in test. This suggests that fine grain (and possibly molding) is less desirable than medium grain (and extrusion?) in graphites for walk-off protection. Such an interpretation of the grain size effect is consistent with the general belief in the graphite industry that coarse-grained graphites have better resistance to thermal shock than fine-grained. [Graphites considered coarse-grained (particle sizes up to several centimeters) were not tested. They may not be

suitable for the sections used (14 to 50 mm thick), as the general consensus is that graphite grain size should be small compared to the dimensions of the part.]

Rather contrary to generalization suggested above is the behavior of the HLM-85 material, a medium-grained extruded material that shattered in test. Why this grade did not perform as well as G-90 and CS is not evident. Tests were made on two samples of HLM-85 cut from the same rod; perhaps additional tests from other lots of this grade might give different results. However, graphites are very complex materials, and there can be many subtle differences in their processing and characteristics.

Table 5-2 does not throw much more light on the differences in test behavior. CS and G-90 were, respectively, the least dense and most dense grades tested, so bulk density (and the corresponding inverse variable, porosity) does not correlate well with good or poor performance in test. Only limited data were found on thermal expansion and thermal conductivity; perhaps the grades that behaved best had lower thermal expansion. Electrical conductivity is listed as a rough indicator of thermal conductivity; no correlation with test behavior is obvious.

Many graphite grades are available besides those tested. Perhaps some further testing of grades with a wider range of characteristics would be worthwhile.

6.   Graphite Cloth

One sample of a "graphite cloth," graphitized polyacrylonitrile, was tested under simulated walk-off conditions. The sample, 0.43-mm (0.017-in.) thick, developed slits and holed through in 30 seconds. Examination by eye and under the microscope (Figure B-33) indicated that the material had not melted, but that woof fibers, especially, had disappeared, presumably by oxidation. Similar results have been reported (Reference 8,9).

If one assumes that multiple layers would behave independently, an assembly of 30 plies, 13-mm (0.5-in.) thick, might last 15 minutes. This is rather speculative in the absence of a multi-layer test. Such a graphite cloth assembly would be considerably lighter than conventional graphite of the same dimensions: 4.5 kg (10 lb) for an aperture plate of the size mentioned above. Material of this type costs about $150/kg ($70/lb), making the cost of material for the plate about $700.

Another approach would be to bond multiple layers of "graphite cloth" together with an organic resin, then heat the composite to carbonize and graphitize the resin. A preliminary test of such material (Reference 8,9) showed marginal performance. Cost would be higher than with unbonded material.

7.   Coated Graphite

Three samples of graphite (grades CS and 3499) were coated with boron nitride, which is white, to evaluate the effect of reducing the solar

absorptance of the material. The boron nitride was in the form of a fine powder dispersed in a water-based binder of aluminum phosphate and applied by spraying, followed by baking. Some graphite support rods were also coated in the same way, for reasons explained below. In test, the white coating disappeared from the area of highest solar flux, and the bare region then spread outward uniformly to areas of lower flux. After this, the samples cracked like uncoated samples of the same grade (Figures B-2 and B-16), except that one CS sample cracked all the way across, rather than half-way (Figure B-10).

Two samples of graphite (grades 8826 and HLM-85) were painted with commercial high-temperature white paints. Their behavior in test was similar to that of samples coated with boron nitride (Figures B-4 and B-28). Table 5-4 compares the performance of graphite samples with and without coatings.

Perhaps the reason that white coatings of high-temperature paint or boron nitride did not significantly improve performance of graphite is that the coatings were lost rather quickly. Why this occurred is not clear; possibilities include melting or decomposition of the coatings at high temperatures, loss of adherence due to differences in thermal expansion, and imperfect initial adhesion. Other coatings might be more successful. In particular, boron nitride is available with other binders (i.e., other than the aluminum phosphate used) and might be applied by other techniques. Aluminum phosphate is not especially high-melting and does not have high thermal conductivity.

B.   SILICON CARBIDE AND SILICON NITRIDE

Two samples of silicon carbide, from different sources, were tested. Both shattered within a second or two (Figures B-34 and B-35). It seems evident that silicon carbide, in the grades tested, is so sensitive to thermal shock failure that it is unsuitable for walk-off protection. Some earlier tests (Reference 16) had given a similar result.

Silicon nitride was not tested, but is not expected to be more resistant to thermal shock, except perhaps in the form of hot-pressed silicon nitride. Such material is relatively expensive and may be difficult to obtain in the sizes needed.

C.   SILICA

Four samples of slip-cast silica and one of fibrous, reaction-bonded silica were tested. A high-purity sample of slip-cast fused silica (SiO_2-JSS-1), with fine particle size, survived 4 minutes and then softened and slumped where it was in contact with the graphite support rods (Figure B-36). This was thought to be an extraneous effect of the test setup and not a fair evaluation of the sample. The sample was therefore retested, turning it over to expose the other side and supporting it with rods that were placed farther from the area of highest solar flux and also were coated with boron nitride (as described above) to reduce the solar absorptance of the rods. This time the silica sample began to slump in the area of highest solar flux, after 1-1/2 minutes of exposure (Figure B-37). At the same time it showed a marked local decrease in solar reflectance, the hot spot appearing

Table 5-4. Effect of White Coatings Upon Performance of
Graphite Samples in Walk-off Tests

Coating Type	Nominal Coating Thickness, mm	Graphite Type	Graphite Thickness, mm	Sample Number	Insolation, W/m^2	Time to Lose Coating, Min:Sec	Fracture During Test	
							Time, Min:Sec	Nature
2500	0.05	8826	25.7	8826-2	730	0:15	1:30	Shattered
None	–	8826	25.7	8826-1	580	–	1:10	Shattered
VHT SP-101	0.05	HLM85	24.	HLM85-2	790	0:20	0:55	Cracked Through
None	–	HLM85	25.7	HLM85-1	730	–	1:25	Shattered
BN, in AlPO$_4$	0.08	3499	25.7	3499-2	700	7:20	8:20	Shattered
None	–	3499	26.0	3499-1	660	–	1:15	Cracked Apart
BN, in AlPO$_4$	0.08	CS	28.1	CS-2	820	6:30	7:55	Cracked Through
None	–	CS	28.1	CS-1	620	–	8:30	Cracked Halfway
BN, in AlPO$_4$	0.04	CS	37.4	CS-6	760	1:40	2:15	Cracked Halfway
None	–	CS	37.2	CS-3	680	–	14:-	Cracked Halfway
None	–	CS	36.2	HB-1	790	–	2:35	Cracked Halfway

black in contrast to the more reflective cooler material around it. A similar sample was tested on both sides; it lasted about 1-1/2 minutes each time before starting to slump and turning locally dark. It is probable that the longer survival in the first test was due to the lower insolation at the time: 670 W/m^2 as compared to 740-790 W/m^2 in the three subsequent tests. This suggests that high-purity slip-cast silica would be satisfactory at somewhat lower flux levels than those used in this test program.

The reflectance of the silica returned upon cooling to near its pre-test value (Figures B-36 through B-39).

If high-purity slip-cast silica survives without softening, it could be the material of choice for walk-off protection because, unlike graphite, it will not oxidize. It has the disadvantages of possible changes in optical properties when heated in service and probable sensitivity to surface dirt and contamination, which may be hard to avoid in field service. Also, the optical transmittance of the silica should be checked out; if too much of the incident sunlight passes through the silica, components behind it will not be adequately shielded. The cost of a segmented aperture plate of high-purity slip-cast silica in the size discussed [25-mm (1-in.) thick, 380-mm (15-in.) ID, and 760-mm (30-in.) OD] would be about $200 in quantities of a hundred or so, or about $12/kg ($6/lb) -- probably affordable.

Two samples of commercial-grade slip-cast silica softened and dripped within 10 seconds (Figures B-40 and B-41). This suggests the importance of high purity and perhaps of crystal structure. These samples had a coarser and less uniform particle size than the high-purity samples and their reflectance was somewhat lower (0.9 versus almost 1.0, Table 2-1). This material would cost about $6/kg ($3/lb); the cost of an aperture shield of the above dimensions would be $40 to $100, depending on the material density chosen.

The fibrous reaction-bonded silica (similar to a proposed second-generation Space Shuttle tile) dripped in less than 10 seconds (Figures 3-3 and B-42). This sample had a black glazed surface toward the incident sunlight that was designed to increase its emittance at elevated temperatures, but also greatly increased its solar absorptance. (The reflectance was roughly 0.05.) Probably the material would have greater resistance to walk-off conditions with a white exposed surface. Though such material might cost $100/kg ($50/lb), its low density means that the required mass would be low, keeping the cost of an aperture plate to perhaps $200.

D.   SILICATES, ALUMINA, ZIRCONIA

All samples of these materials melted rather quickly. The sample that lasted the longest was of fibrous zirconia, about 25-mm (1-in.) thick, which melted in 1 minute (Figure B-55). A zirconia sample of similar thickness had been cast from a powder-vehicle mixture and then sintered; it melted in 17 seconds (Figure B-54). A sample of zirconia cloth 0.5-mm (0.02-in.) thick developed slits in 8 seconds (Figure B-56).

The alumina samples were in the form of "paper" (felt) 1.5-mm (0.06-in.) thick and less. All melted within 6 seconds (Figures B-51 through B-53).

Silicate samples tested included three of mullite and one of processed kaolin (both alumina-silica), one of cordierite (magnesia-alumina-silica), and two of alumina-boria-silica, in various shapes. All melted within 4 seconds (Figures B-43 through B-49).

These refractory oxides melted at times shorter than those at which high-purity silica softened and slumped, even though their melting temperatures are higher than the glass transition point of silica. Thus, other characteristics must be important in determining behavior in these solar tests (the absorptance/emittance ratio, internal radiative heat transfer, etc.)

E.   COATED COPPER AND ALUMINUM

A copper sample 25-mm (1.0 in.) thick was nickel-plated and painted with a commercial high-temperature white paint. It began to melt (Figure B-57) in two minutes. After this test, the paint was removed and the sample repainted with another brand of commercial high-temperature paint, white on one side and black on the other. It was then tested two more times, once with the black side facing the concentrated sunlight and once with the white side facing the sunlight. The sample was placed so that the area of maximum solar flux fell on a different part of the sample in each of the three tests. With the repainted white face exposed, melting started in 3 minutes; with the black face exposed, in 1 minute (Figures B-58,B-59 and Table 5-5). The shorter survival time with the black paint is presumably due to the difference in solar absorptance between black and white paints (reflectance 0.06 and from 0.6 to 0.8, respectively). The difference in survival time with the two white paints may also be due to absorptance; the white giving longer survival had the higher reflectance.

A test was run on an aluminum alloy sample 1.8-mm (0.07-in.) thick coated on both sides with a laboratory-produced inorganic white paint developed for use on spacecraft. It melted in about 1/2 second (Figure B-60). A thermocouple had been attached to the center of the face away from the sunlight (Figure 4-2). The maximum temperature recorded before the sample fell apart was 200°C (400°F). This low temperature presumably indicates that the thermocouple temperature lagged behind that of the aluminum sample and did not represent the latter. [The melting range (solidus to liquidus) of this alloy is 580 to 650°C, 1080 to 1200°F.]

F.   STEEL

A sample of stainless steel screen 2-mm (0.4-in.) thick melted in 2 seconds (Figure B-61).

G.   POLYTETRAFLUOROETHYLENE

Polytetrafluoroethylene was tested as an ablative material. It was chosen with the thought that it would ablate to gas without going through a liquid phase; this did not happen. Within a second of starting simulated walk-off exposure, small pieces or droplets popped off with noticeable noise, leaving rounded pits (Figure B-62). The popping may have been caused by

Table 5-5. Effect of Coatings on Performance of Copper Sample in Walk-Off Tests

Coating Color	Coating Type	Nominal Coating Thickness, mm	Copper Thickness, mm	Sample Number	Insola- tion, W/m^2	Time to Lose Coating, Min:Sec	Melted – Time, Min:Sec
Flat White	VHT SP-101	0.05	25.6	Cu-1	780	Not lost	2:00
White	2500	0.05	25.6	Cu-1/2	720	Not lost	2:50[a]
Flat Black	2500	0.05	25.6	Cu-1/3	690	0:30	0:50

[a]Melting may have been initiated by hot support rod.

inclusions or other light-absorbing defects just under the surface that generated hot gas locally. When testing was resumed, copious black smoke evolved and melting was observed after 2 minutes (Figure B-63). In a further test on this sample, the remaining 18 mm (0.7 in.) of thickness melted through after an additional 6 minutes of exposure (Figure B-64). Because of the melting and dripping, as well as the smoke which could deposit on mirrors and other collector surfaces, polytetrafluoroethylene appears unsuitable for walk-off protection.

H. COMPARISON OF MATERIALS

Comparison of the behavior of the various materials in the walk-off tests emphasizes the importance of the melting point: The only materials tested that did not melt or slump were graphite and silicon carbide. Neither of these materials melts at atmospheric pressure.

Comparing silicon carbide with graphite, silicon carbide was unsatisfactory because it shattered in thermal shock. Silicon carbide has lower thermal conductivity than graphite, which is doubtless a major factor in its performance.

Behavior of the various graphite grades was compared earlier in this report.

SECTION VI

WALK-OFF TESTS: OXIDATION RESULTS AND DISCUSSION

During walk-off tests the graphite samples lost significant thickness at the center of their exposed faces, with a corresponding loss in mass. Table 6-1 gives the raw data on these losses for graphite grades CS and G-90 and also the data normalized to an exposure time of 15 minutes. The percentage mass losses were also normalized to a standard sample size, 25 x 200 x 200 mm (1 x 8 x 8 in.), assuming that the mass loss in grams is independent of sample size. This assumption seems reasonable because the thickness loss is primarily near the center of the exposed spot.

The loss in thickness due to oxidation for grades CS and G-90 varied from 0.2 mm (0.008 in.) to 8 mm (0.3 in.) per 15-minute exposure. The corresponding loss in mass, normalized, was 2 to 22% (Table 6-1). This amount will probably be acceptable for walk-off protection because walk-off is expected to be an infrequent event and the test was probably more severe than the expected service. (In test, the spot of maximum solar flux was held fixed on the sample, whereas in walk-off it would traverse across the shield. This should reduce maximum temperature and oxidation rate.) An aperture plate or shield could perhaps be replaced after a few walk-offs.

The effect of wind speed on the oxidation loss was significant (Figure 6-1) and accounts for a large part of the variation in loss between samples. For grades CS and G-90, the correlation coefficient equals 0.83 (t=5.7, degrees of freedom (d.f.) = 15, significant at 0.01 level; percent of variance attributable to wind speed is 68%).

Interestingly, insolation did not have a significant effect upon mass loss rate (t=0.88, d.f. 15, not significant at 0.05 level). The literature indicates that at the temperatures encountered in walk-off, the rate-limiting process is mass transfer through the boundary layer (References 20,21). Insolation level would be expected to have only a small effect on mass transfer, whereas wind speed would have a major effect: Wind brings oxygen and removes carbon monoxide and carbon dioxide from the reacting surface.

Figure 6-1 also suggests that the mass loss rate for grade CS graphite was somewhat lower than that for grade G-90 under comparable conditions. The difference, however, is not statistically significant (t=1.74, d.f. 15, not significant at 0.05 level). Likewise, examination of the data suggests that the loss rate was greater during retest than during the first test of each sample, and that boron nitride coating and prior immersion in water reduce the oxidation rate, but none of these changes had a statistically significant effect based on the measurements made.

The 10-mm (3/8-in.) diameter support rods (graphite grades 580, 873S, and HC) oxidized completely away within 15 minutes in strong winds, at solar fluxes of about 3000 kW/m^2 -- a more rapid loss than encountered for the flat test samples (Figure B-65). When the wind was light, little oxidation of the rods was observed. Radius of curvature and thickness thus affect the oxidation rate of graphites exposed to walk-off conditions.

Table 6-1. Weight and Thickness Loss for Graphite Samples,
Grade G-90 and CS, in Walk-off Tests

Normalized to 15-Minute Exposure.
Mass loss also normalized from sample size
before first test to 25 x 200 x 200 mm.

Grade	Sample Number	Notes[a]	Dimensions Before First Test, mm	Test Duration, min:sec	Inso-lation, W/m^2	Lost in Test Thickness, mm Measured	Normalized	Mass, % Measured	Normalized	Avg. Wind Speed, m/sec
CS	HB-1	12,14	36.2 x 153 x 203	2:40	790	0.3	–	1.6	–	1
CS	HB-1/2	4,11	36.2 x 153 x 203	14:00	840	7.9	8.5	8.5	10.2	5
CS	CS-1	–	28.1 x 205 x 205	9:40	620	0.4	0.6	3.4	5.8	3
CS	CS-1/2	11	28.1 x 205 x 205	8:00	830	2.2	4.1	3.2	7.1	2
CS	CS-1/3&4	11,18	28.1 x 205 x 205	27:20	880	4.7	2.9	13.1	8.5	3
CS	CS-2	1	28.1 x 205 x 205	8:00	820	0.1	0.2	0.8	1.8	3
CS	CS-3	–	37.2 x 207 x 207	15:00	680	5	5	9.3	14.8	7
CS	CS-3/2	11	37.2 x 207 x 207	15:00	670	4	4	9.8	15.6	11
CS	CS-4	7	36.7 x 207 x 207	15:00	800	8	8	9.2	14.5	10
CS	CS-4/2	11	36.7 x 207 x 207	15:00	780	2	2	14.1	22.2	9
CS	CS-6	1	37.4 x 207 x 207	15:00	760	2.6	2.6	5.2	8.3	5
CS	CS-8	–	13.5 x 204 x 204	15:00	670	2.3	2.3	15.8	8.9	4
CS	CS-9	–	26.3 x 204 x 204	15:00	840	2.9	2.9	7.7	8.4	3
CS	CS-10	–	50.6 x 203 x 204	15:00	680	2.4	2.4	5.8	12.2	6
CS	CS-12	–	50.7 x 203 x 204	15:00	880	2.4	1.8	4.0	8.4	4
G-90	G90-1	14	24.5 x 155 Dia.	15:00	770	0.6	0.6	5.3	2.5	2
G-90	G90-1/2	11	24.5 x 155 Dia.	15:00	770	3.0	3.0	15.2	7.0	4
G-90	G90-2	7,14,19	25.0 x 155 Dia.	11:10	870	2.1	2.7	10.9	6.9	6

[a] See Table 2-1.
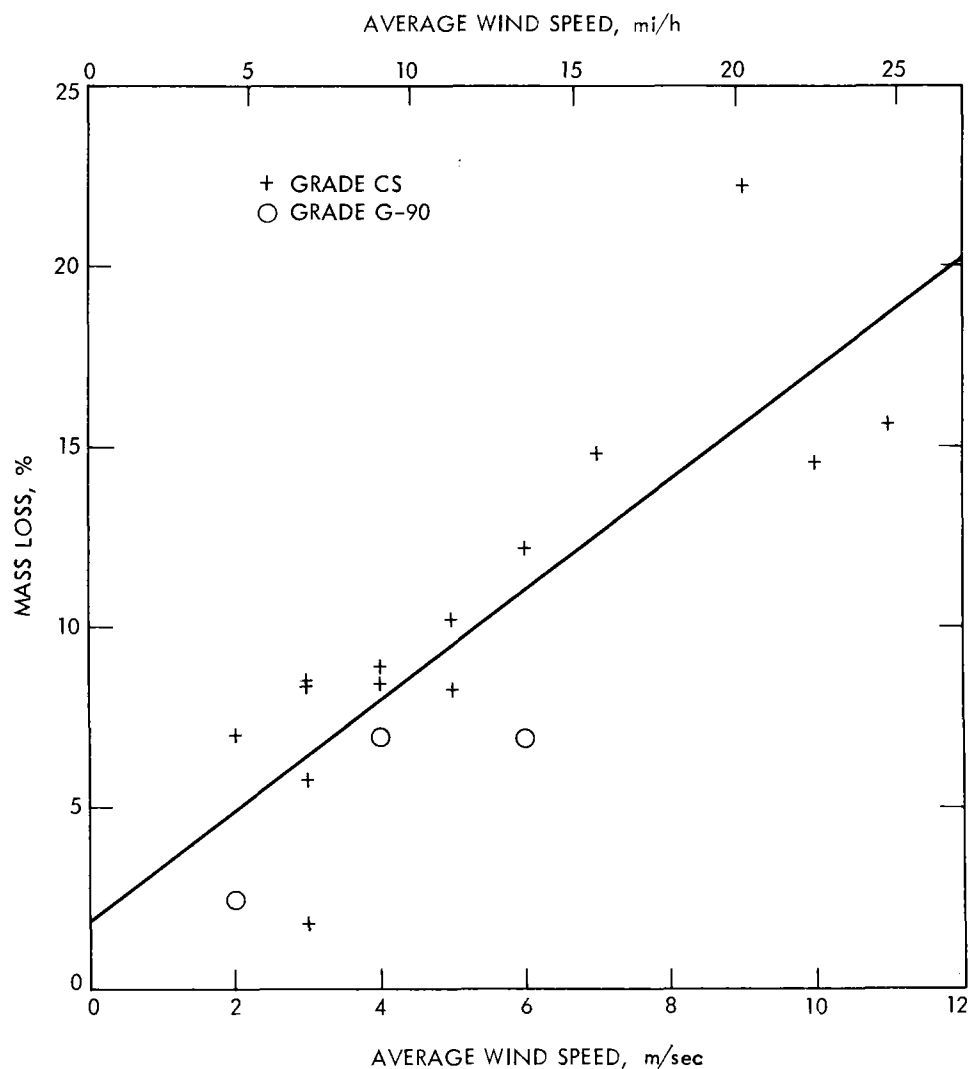
Figure 6-1. Effect of Wind Speed on Mass Loss by Oxidation
for Graphite Grades CS and G-90 in Walk-off
Tests. [Mass losses normalized to 15 minutes
exposure and 25 x 200 x 200 mm (1 x 8 x 8 in.)
sample. Samples exposed less than 3 minutes
between interruptions are not plotted. Line
is least-squares fit.]

The lower inner edge of the more massive test fixture, which initially had an angle of 135 degrees and was rounded to a radius of 3 mm (0.12 in.), lost 4.0 mm (0.16 in.) during a total exposure of 13 hours at solar fluxes of roughly 100 kW/m^2 plus additional heat transferred from the samples (Figure 3-4). Some of this loss was probably due to erosion through chemical reaction with samples that melted.

SECTION VII

ACQUISITION TESTS: RESULTS

The repeated on-sun/off-sun cycles used for some samples of grade CS graphite (samples CS-5, CS-7, CS-7/2; Figs. B-15, B-17, B-18) give an indication of the extent of graphite oxidation during frequent normal sun acquisitions and deacquisitions. Results appear in Table 2-2. In 700 to 2000 cycles, which might represent a year or two of service, the samples lost 5 to 7 mm in thickness and 0.15 to 0.2% of their weight (normalized to a thickness of 25 mm, 1 in.). This appears to be tolerable. The insolation in these tests was 780 to 960 W/m^2; acquisition and deacquisition in service probably would be primarily at low sun elevation, when insolation would be lower. Also, the tests were severe in that the spot of concentrated sunlight remained at a fixed position on the sample; in acquisition-deacquisition the spot would traverse the material. The graphite in the spot reached a steady-state temperature of 650 to 700°C (1200 to 1300°F) when off the sun (sample CS-5), whereas after a single acquisition or deacquisition, it would cool to near ambient temperature. Wind speed during the simulated acquisition/deacquisition test was 2 to 10 m/s, 4.5 to 22 mi/h, representative of the wind conditions likely to be encountered during operation.

SECTION VIII

SPILLAGE TESTS: RESULTS

The various positions of the sample edge in the spillage tests were used to indicate the temperatures attained by the lip of a graphite aperture plate on which spillage impinges during normal solar operation. In particular, the test of sample CS-13 represented, approximately, the conditions that were planned for the organic Rankine receiver with an aperture diameter of from 350 to 380 mm (14 to 15 in.; see Table 3-1). The edge temperature reached was only 107°C (225°F; Table 2-3). At this temperature, according to available data, the oxidation of graphite would be negligible even over periods of many years (Reference 20,21).

Tests of samples CS-13/4, CS-13/2, and CS-13/3 represented conditions on receiver aperture plates having diameters of 150, 200, and 250 mm (6, 8, and 10 in.), positioned close to the focal plane (Table 3-1). Temperatures reached were, respectively, 312, 173, and 133°C (594, 343, and 271°F). (See Figure B-25.) Figure 8-1 is a plot of the calculated oxidation rate for grade CS graphite, extrapolated from higher temperature data (Reference 22). For the 200 and 250 mm (8 and 10 in.) apertures, the oxidation rate is negligible; for 150 mm (6 in.), the calculated rate of 1.5 g/m²-y certainly appears acceptable.

In utilizing the results in Table 2-3 for various collector designs, the governing parameter is the flux density on the edge or lip of the sample or aperture plate. This value should be known for each collector design. Figure 8-2 is a plot of the steady-state temperature versus the flux density at the edge. [The correlation coefficient is 0.93; the correlation is significant at the 0.01 level (t=4.9, d.f.=4).] Figure 8-3 is a corresponding plot with the flux density expressed as a percentage of the peak flux density in its plane perpendicular to the optical axis. [Here the correlation coefficient is 0.98, and is significant at the 0.01 level (t=10.9, d.f.=4).] For the usual assumption that the flux density in this plane may be represented as a two-dimensional Gaussian distribution, the flux density at the lip, expressed as a percentage of the peak, is equal to the percent spillage [100 x (1 minus the intercept factor)] if the flux distribution is centered in the receiver aperture. For spillage up to 2%, which is representative, the edge temperature (Figure 8-3) should not exceed 220°C and the corresponding loss of graphite by oxidation (Figure 8-1) should be negligible even over periods of years. This is not true at spillage over 6% when the edge temperature may reach 400°C or more, but such high spillage loss is unlikely to be considered tolerable.

According to the literature, graphite oxidation at temperatures up to 750 to 850°C (1400 to 1600°F) is reaction-rate limited (References 20, 21, 23). Loss rates due to spillage, therefore, should not be significantly affected by wind speed.
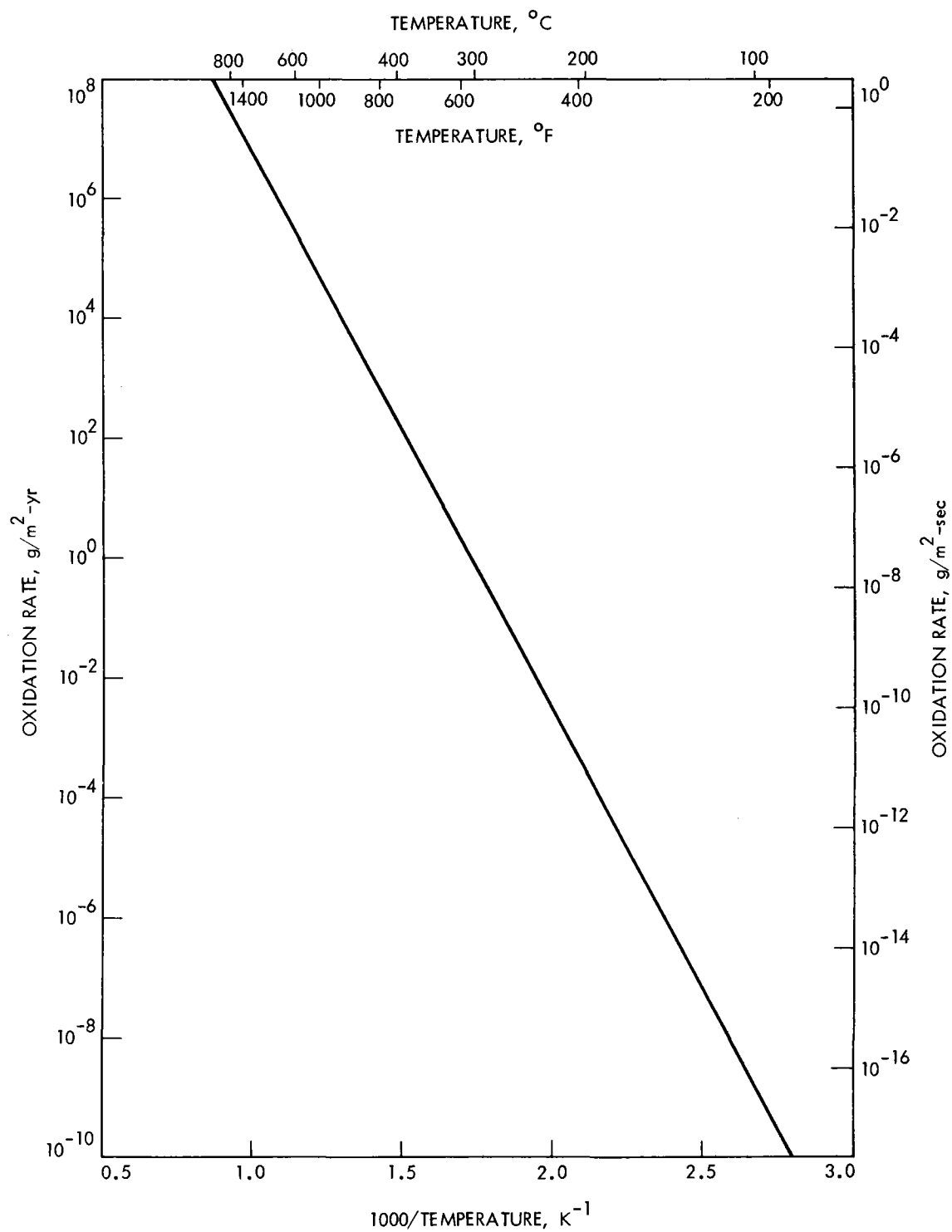
Figure 8-1. Calculated Oxidation Rate Versus Temperature for Grade CS Graphite (Based Upon Data in Reference 19)
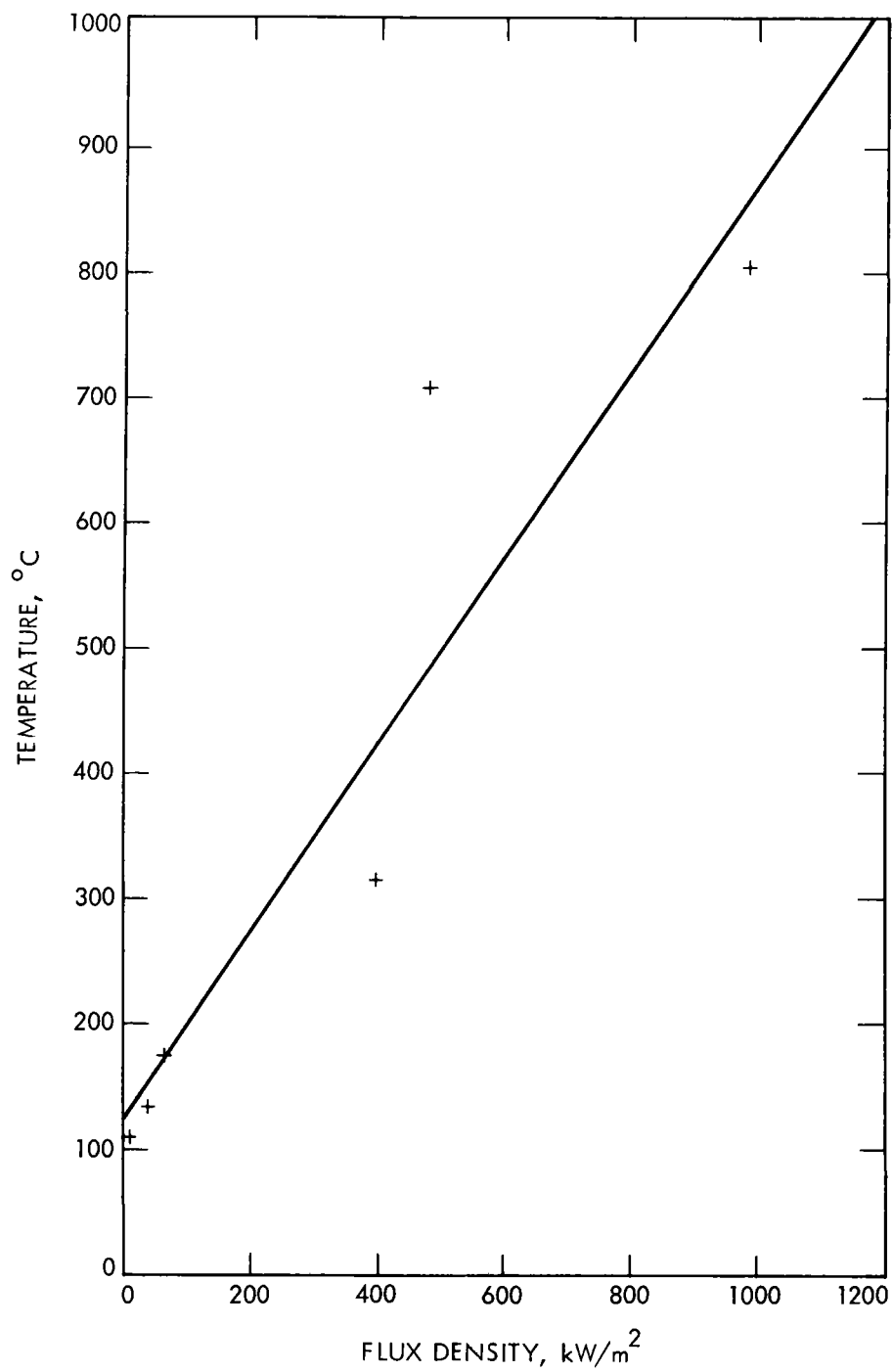
Figure 8-2. Temperature in Spillage Test Versus Flux Density at Edge of Graphite Sample. (Line is least-squares fit.)
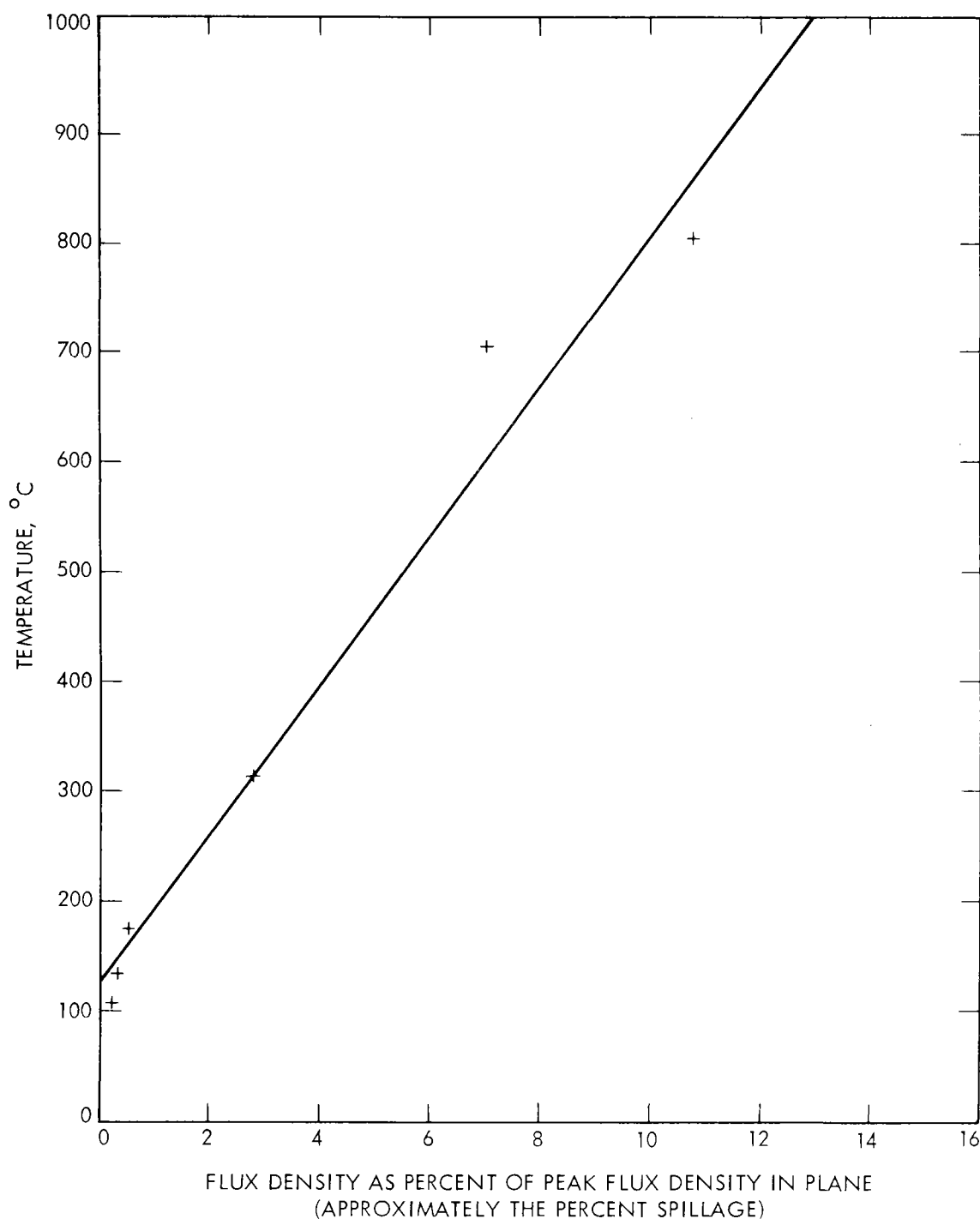
Figure 8-3.   Temperature in Spillage Test Versus Flux Density
at Edge of Sample. (Expressed as percent of peak
flux density in plane normal to optical axis.
This percentage equals the percent spillage if
one assumes that the flux distribution in the
plane is Gaussian and centered in the receiver
aperture. Line is least-squares fit.)

SECTION IX

RECOMMENDATIONS

For aperture plates to passively withstand walk-off under the conditions simulated and for similar applications, the material of choice appears to be graphite, grade G90 or CS. Some other conventional graphites with medium grain size will probably also be satisfactory, but testing will be needed to identify them. Segmenting is probably desirable to reduce thermal stress and reduce replacement cost. The directional properties of the graphites should be considered in the design, as should the heating by spillage and associated long-term oxidation. For any specific receiver design, an aperture plate or plates should be fabricated and tested under walk-off and other conditions.

Another promising possibility is graphite cloth in multiple layers. Further testing would be needed to define its usefulness. It will not fracture, but would probably have to be replaced after each walk-off. Its resistance to oxidation during acquisition/deacquisition and spillage remains to be determined.

Finally, high-purity slip-cast silica and possibly white fibrous silica might be considered for applications where the walk-off flux density does not exceed 4000 kW/m^2. Such materials would not suffer from oxidation during acquisition/deacquisition or spillage, but their optical transmittance and their sensitivity to effects of surface dirt likely to be deposited in field service would need to be checked.

Of the recommended materials, a graphite grade such as CS would be the least expensive.

REFERENCES

1. L.D. Jaffe, R.R. Levin, P.I. Moynihan, B.J. Nesmith, W.A. Owen, E.J. Roschke, M.K. Selcuk, D.J. Starkey, and T.O. Thostesen, "Systems Approach to Walk-off Problems for Dish-Type Solar Thermal Power Systems," JPL Doc. 5105-97, Aug. 21, 1981, and <u>Proc. Intersociety Energy Conversion Engineering Conf.</u>, Orlando, FL, Aug. 1983, Am. Soc. Chem. Eng.

2. J. D. Walton and C. Royere, "Evaluating The Thermal Shock Resistance of Ceramics in a Radiant Thermal Energy Environment," <u>Science of Ceramics 7</u>, 219-236, 1973.

3. J. D. Walton, Jr., S. H. Bomar, Jr., and H. L. Bassett, "Evaluation of Materials in a High Heat Flux Radiant Thermal Energy Environment 'U'," Georgia Institute of Technology, Engineering Experiment Station, Final Report AMMRC CTR 73-6 to Army Materials and Mechanics Research Center, May 1973.

4. J. D. Walton, Jr., S. H. Bomar, Jr., J. A. Fuller, and J. N. Harris, "Materials for Hardened Phased-Array Antennas," Georgia Institute of Technology, Engineering Experiment Station, Report AMMRC TR 81-44 to Army Materials Research Center, September 1981.

5. S. H. Bomar, et al, Georgia Institute of Technology, Engineering Experiment Station.

6. L. K. Matthews and G. P. Mulholland, "High Temperature High Flux Material Testing for Solar Flux Applications," <u>Solar Energy 23</u>, 175-181, 1979.

7. H. Le Doussal, J. P. Carrie, M. Chastant, L. Halm, M. Jon, C. Royere and J. L. Tuhault, "Comportement des produits refractaires soumis a des sollicitations thermomechanique severes," <u>Bull. Soc. Fr. Ceram.</u>, No. 124, pp 29-55, July-Sept. 1979.

8. H. Bank and W. Owen, Internal communication, JPL, 1980.

9. R. Smoak, Internal communication, JPL, 1980.

10. R. L. Pons and A. F. Dugan, "A Small Community Solar Thermal Power System," <u>Solar Sciences 1</u>, No. 1, 15-35. (Spring 1982).

11. R. L. Pons and F. P. Boda, "Preliminary Tests Results for The Small Community Solar Power System," Paper ASME 82-WA/Sol-30, ASME Winter Annual Meeting, Solar Energy Division, Phoenix, AZ, November 1982.

12. V. R. Goldberg, "Test Bed Concentrator (TBC)," in <u>Proc. 1st Semiannual Distributed Receiver Systems Program Review</u>, Report DOE/JPL-1060-23, pp 35-39, April 1980.

13. M. J. Argoud, "Test Bed Concentrator Mirrors," ibid, pp 41-46.

14. D. J. Starkey, "Initial Test Bed Concentrator Characterization," ibid, pp 47-51.

15. W. J. Carley, "Progress in Point Focusing Solar Concentrator Development at JPL," _Proc. 1980 Annual Meeting, American Section, International Solar Energy Soc._, Phoenix, AZ, June 1980.

16. D. J. Starkey, "Characterization of Point Focusing Test Bed Concentrator at JPL," in _Parabolic Dish Solar Thermal Power Annual Review Proc._ Report DOE/JPL 1060-46, pp 135-142, May 1981.

17. D. J. Starkey and W. A. Owen, "The JPL Flux Mapper and the Characterization of Point Focusing Test Bed Concentrators at JPL," _Proc. 1981 Annual Meeting, American Section, International Solar Energy Soc._, Atlanta, GA, June 1981, pp 351-356.

18. W. A. Owen, Internal communications, JPL, 1981-1983.

19. E. W. Dennison, Internal communication, JPL, 1983.

20. F. K. Earp and M. W. Hill, "Oxidation of Carbon and Graphite," Conf. on Industrial Carbon and Graphite, London, 1957, pp 326-333.

21. E. A. Gulbransen, K. F. Andrew, and F. A. Brossert, "Oxidation of Graphite at Temperatures of 600° to 1500°C and at Pressures of 2 to 76 Torr of Oxygen," _Jnl. Electrochemical Soc._, 110, pp 476-483, 1963.

22. Carbon Products Division, Union Carbide Corp., "Oxidation of CS-312 in Dry Air," Union Carbide Corp., Palma, Ohio.

23. D. D. Knight and E. D. Knecktel, "Graphite Oxidation at Low Temperatures in Subsonic Air," AIAA Paper 73-735, 8th Thermophysics Conference, Am. Institute of Aeronautics and Astronautics, Palm Springs, CA, 1973.

APPENDIX A

MATERIALS AND SAMPLE PREPARATION

Bulk densities and approximate reflectances of samples are listed in Table 2-1.

A.   GRAPHITE

Other characteristics of the graphites used are listed in Table 5-2. Sources of the material are as follows:

(1)   Grade 580. Used for support rods only. Manufactured by Airco Carbon Division of Airco, Inc.; supplied by Graphite & Specialty Products, Inc.

(2)   Grades 3499 and 8826. Manufactured by Airco Carbon. Test samples supplied by Airco Carbon. Test fixture (Grade 3499) supplied by Graphite & Specialty Products Inc.

(3)   Grade 8735. Used for support rods only. Manufactured by Airco Carbon; supplied by Graphite & Specialty Products Inc.

(4)   Grade CS. Manufactured by Carbon Products Division of Union Carbide Corp. Two samples supplied by Union Carbide. One sample supplied through J. Woodbury and H. Bank of JPL. Eleven samples supplied by Graphite & Specialty Products.

(5)   Grade HC. Used for support rods only. Manufactured and supplied by Graphite Products Division of Great Lakes Carbon Corp.

(6)   Grade HLM-85. Manufactured and supplied by Great Lakes Carbon. Supplied through J. A. Barry of JPL.

(7)   Grade G-90. Manufactured and supplied by Carborundum Specialty Graphite Products, Kennecott Corp. Supplied through J. A. Barry of JPL.

(8)   Cloth. Pluton B-1. Polyacrylonitrile cloth, oxidized, carbonized, stretched, graphitized at about 2000°C. Fiber properties:

Filament size	8 μm
Density	1.8 Mg/m^3
Thermal conductivity	70 $W/m°C$

Manufactured by 3-M, Inc. Supplied through David Lawson of JPL. Cost in quantity is about $150/kg ($70/lb).

B.   SILICON CARBIDE

    (1)   Honeycomb. Alpha silicon carbide, reaction-bonded, honeycomb. Manufactured by NGK (Nippon Gaishi Kaishya, "Japan Insulator Company," a subsidiary of Noritake); supplied by Sanders Associates, Inc., through W.A. Owen of JPL.

    (2)   Plate. Sintered, recrystallized silicon carbide, grade NC-400, made from bimodal powder, containing small amounts of carbon and silicon. Not impregnated with silicon. Mostly alpha. Manufactured by Norton Company; supplied by AiResearch Manufacturing Company through W. A. Owen of JPL.

C.   SILICA

    (1)   Slip cast, high purity. Rebonded fused silica: slip cast and sintered. Slip of deionized water plus silica powder. Mean particle size of powder 7.8 μm; maximum particle size 44 mm. Typical composition of powder (weight percent):

Fe_2O_3	0.003
Al_2O_3	0.23
CaO	0.001
MgO	0.007
TiO_2	0.002
Cr_2O_3	0.001
CoO	< 0.001
Na,K,Li	10 ppm each
SiO_2	99.76 (by difference)

Crystal structure of sample: sun face 1/2 to 1% crystobalite; remainder glassy. Interior believed all glassy.

Slip cast and sintered by Engineering Experiment Station, Georgia Institute of Technology, from powder manufactured by Thermal Materials Corp. Samples supplied by Georgia Institute of Technology; one through J.A. Stearns of JPL. Cost in quantity is about $12/kg ($6/lb).

    (2)   Slip cast, commercial purity.

        (a)   Higher density material. Rebonded fused silica ("Masrock"); slip cast and sintered from silica powder. Powder mixture of 0.30 mm particles and > 8 μm particles.

Typical properties:

Bulk density	1.8 to 1.9 Mg/m^3
Apparent porosity	11 to 15%
Crushing strength	60 MPa
Modulus of rupture	10 to 15 MPa
Coefficient of thermal expansion (mean, 25 to 1000°C)	0.7 x 10^{-6} °C^{-1}

Composition (weight percent):

Fe_2O_3	0.05
Al_2O_3	0.25
CaO	0.03
MgO	0.02
Na,K,Li,as oxides	0.02 total
SiO_2	99.63

Manufactured by Harbison-Walker Refractories, Dresser Industries, Inc; supplied by United Stirling, Inc. Cost in quantity is about $6/kg ($3/lb).

(b)   Lower density material. Rebonded fused silica ("Fusil Foam 50"); slip cast from silica powder with foaming agent, sintered.

Typical properties:

Bulk density	0.83 Mg/m^3
Apparent porosity	63%
Crushing strength	8.3 MPa
Modulus of rupture	3.6 MPa
Thermal conductivity (at 480°C)	4.8 W/m°C
Coefficient of thermal expansion (mean, 25 to 1000°C)	0.7 x 10^{-6} °C^{-1}

Composition (percent):

Fe_2O_3	0.03
Al_2O_3	0.2

A-3

CaO,MgO	0.03
K_2O,Na_2O	0.02
SiO_2	99.6

Manufactured by Harbison-Walker Refractories; supplied by United Stirling, Inc. Cost in quantity is about \$6/kg (\$3/lb).

(3) Fibrous. Silica fibers, fusion bonded with boron-rich oxides ("Fibrous Refractory Composite Insulation, FRCI-12"). Surface exposed to concentrated sunlight was glazed with "Reaction Cured Glass" (14 MIL RCG Class 2). Nominal glaze composition (weight percent):

SiO_2	92
B_2O_3	6
SiB_4	2

Manufactured and supplied by Lockheed Missiles and Space Company. Cost in quantity is about \$100/kg (\$50/lb).

D. SILICATE

(1) Mullite, Fine Honeycomb. Alumina/silica mole ratio approximately 3:2. Also contains aluminum titanate. Manufactured by Corning Glass Corp.; supplied by Sanders Associates through W.A. Owen of JPL.

(2) Mullite, Coarse Honeycomb. Alumina/silica molé ratio approximately 3:2.

Typical properties:

Bulk density	0.57 g/cm^3
Porosity	0.154 cm^3/g
Melting point	1780°C
Specific heat	0.15 cal/g^{o}C
Thermal conductivity	6.7 W/m^{o}C
Coefficient of thermal expansion (at 750°C)	4.5×10^{-6} $^oC^{-1}$
Bending strength	59 MPa

Tensile strength   38 MPa

Young's modulus   45 GPa

Composition (weight percent):

Al$_2$O$_3$ 65.9

SiO$_2$ 32.1

Others   2.0

Manufactured by NGK; supplied by Sanders Associates through W.A. Owen of JPL.

(3) Processed Kaolin Fibrous Board. "M Board," vacuum-formed from slurry of fibers made from kaolin, alumina-silica fireclay, plus binders including organics.

Typical properties:

Density   0.24 Mg/m^3

Melting point   1760°C

Thermal conductivity at
    mean temperature 540°C   2.2 W/m^{o}C

Compressive strength   0.17 MPa

Modulus of rupture   0.69 MPa

Composition (percent):

Al$_2$O$_3$ 41.0

SiO$_2$ 52.1

Organics   4 to 7

Manufactured by Babcock & Wilcox Company; supplied through Wayne Phillips of JPL. Cost in quantity is about $3.50/kg ($1.50/lb).

(4) Cordierite Honeycomb. Extruded blend of clay, talc, and alumina, plus binders and lubricants, then sintered. Structure: cordierite plus traces of spinel and corundum.

Typical properties:

Density (nominal)   0.47 Mg/m^3

Melting point   1470°C

Specific heat	0.19 cal/g$^\circ$C	
Thermal conductivity	4.2 W/m$^\circ$C	
Coefficient of thermal expansion (at 750°C)	2.0×10^{-6} $^\circ$C^{-1}	
Nominal composition	2 MgO $\cdot$ 2 Al$_2$O$_3$ $\cdot$ 5 SiO$_2$	

Manufactured by Corning Glass Works; supplied through Maurice Argoud of JPL.

(5) Alumina-Boria-Silica Cloth. "Nextel 312" cloth.

Filament properties:

Filament density	2.7 Mg/m^3
Solidus	1700°C
Liquidus	1800°C
Filament modulus of elasticity	152 GN/m^2
Filament tensile strength	1720 MN/m^2

Cloth properties:

Type	5H-26	5H-40
Thread count, cm^{-1}	11 x 10	13 x 8
Yarn type	1/2; 1/2	1/4; 2/2
Weave	5 Harness Satin	
Nominal thickness, mm	0.66	0.99
Nominal mass, g/m^2	407	854
Breaking strength, without sizing, N/cm	500	210
Thermal conductance at 600°C, W/m^2 $^\circ$C	---	140

Composition (weight percent):

Al$_2$O$_3$	62
B$_2$O$_3$	14
SiO$_2$	24

Manufactured by 3-M, Inc. Supplied by Babcock & Wilcox through United Stirling, Inc. Cost in quantity is about $125/kg ($60/lb).

E.   ALUMINA

APA-3 Paper. Paper made from alumina ("SAFFIL") fibers with alumina binder.

Fiber properties:

Fiber density	3.4 Mg/m^3
Mean diameter	3 μm
Tensile strength	1000 MPa
Melting point	2040 ^oC (3700^oF)

Paper properties:

Color	White
Breaking strength (1 ply)	1.4 N/mm of width

Composition (weight percent):

Al_2O_3	96
SiO_2	4

One sample of paper was coated with rigidizer consisting of 28 weight percent of alumina (99% purity) in a water base. After coating, this material was baked 5 minutes at 93^oC (200^oF) and 5 minutes at 260^oC (500^oF). Manufactured by Zircar Products, Inc.; supplied by United Stirling, Inc.

F.   ZIRCONIA

(1)   Grade 0872, Cast. Made from ZrO_2 partially stabilized with 3 to 3 1/2 weight percent of CaO. Cast from a mixture of coarse-grained powder with a vehicle and sintered above 1680^oC (3050^oF). Color: pale yellow.

Manufactured and supplied by Zircoa Products Division, Corning Glass Company; supplied through J.A. Stearns of JPL.

(2) Grade ZYFB6, Fibrous Board. Board made of fibers, without binder.

Fiber properties:

Diameter	4 to 6 μm
Fiber density	5.6 to 5.9 Mg/m^3
Stabilizer	Y_2O_3
Composition (weight percent)	
ZrO_2 + HfO_2 + Y_2O_3	>99
Crystal structure	Cubic
Melting point	2600°C (4700°F)

Board properties:

Bulk density	0.96 Mg/m^3
Porosity	84%
Flexural strength	2 MPa
Color	White

Manufactured and supplied by Zircar Products, Inc.; supplied through J. Woodbury of JPL.

(3) Grade ZYW30A, Cloth. Cloth woven from zirconia fibers.

Fiber properties:

Diameter	4 to 6 μm
Fiber density	5.6 to 5.9 Mg/m^3
Composition (weight percent):	
Y_2O_3 (stabilized)	8
ZrO_2 + HfO_2 + Y_2O_3	>99
Crystal structure	Cubic + tetragonal
Melting point	2600°C (4700°F)

Cloth properties:

Weave	Satin
Bulk density	1.0 Mg/m^3
Porosity	83%
Breaking strength	0.7 N/mm of width
Color	White

G. COPPER

Electrolytic. Electrolytic copper, plate, Federal Specificiation QQ-C-576. Melting point 1083°C (1980°F).

H. ALUMINUM

T6061

Density	2.70 Mg/m^3
Melting point	582°C (1080°F, solidus) to 652°C (1205°F, liquidus)

Composition (weight percent):

Mg	1.0
Si	0.6
Cu	0.25
Cr	0.25
Al	Balance

Supplied by Illinois Institute of Technology Research Institute through Kudret Selcuk of JPL.

I. STEEL

Woven wire mesh of austenitic stainless steel. Wire diameter 0.1 mm (0.039 in.), mesh 2.2 strands/cm (5.6/in.). Melting range 1400-1450°C (2550-2650°F).

Nominal composition (weight percent):

Chromium	19
Nickel	9
Carbon	0.08 max
Manganese	2 max
Silicon	1 max
Iron	Balance

Supplied by United Stirling, Inc.

J.   POLYTETRAFLUOROETHYLENE

Polytetrafluoroethylene plate - supplied by Plastics Center, Inc. Cost in quantity is about $10/kg ($5/lb).

K.   BORON NITRIDE COATING

This coating material ("Series A") consists of boron nitride powder (75 to 90%) and an aluminum phosphate binder (25 to 10%) in a water-base suspension. The coating was air-dried, then oven-dried 2 hours at 65-95°C (150-200°F), then heated to 800°C (1500°F).

Manufactured and supplied by Electric Products Division, Carborundum Company.

L.   HIGH TEMPERATURE PAINTS

(1)   Series 2500, White and Flat Black. "Pyromark". Binder: blend of #805 and #806A silicone resins (Dow Corning). White pigment: believed to be primarily TiO_2.

On copper, applied over nickel electroplate (Federal Specificiation QQ-N-290, class 1 grade G). On graphite, applied without undercoat on side exposed to concentrated sunlight and on edges. Two coats applied. Coating air dried, then oven baked 2 hours at 250°C (480°F), heated to 540°C (1000°F), and held 15 minutes.

Manufactured and supplied by Tempil Division, Big Three Industries, Inc.

(2)   VHT SP-101, Flat White. Binder: silicone resins modified. Pigment: believed to be primarily TiO_2. Thinner: toluene and acetone.

On copper, applied over nickel electroplate (Federal Specification QQ-N-290, class 1 grade G). On graphite, applied without undercoat. Coating air-dried, then heated 15 minutes at 120°C (250°F), 30 minutes at 315°C (600°F), 60 minutes at 425°C (800°F), and 30 minutes at 540°C (1000°C).

Manufactured and supplied by Sperex Corp.

(3) Zinc Orthotitanate. Binder: potassium silicate. Pigment: zinc orthotitanate. Thinner: distilled water. Emittance at 25°C: 0.91.

Made and supplied by Illinois Institute of Technology Research Institute through Kudret Selcuk of JPL.

APPENDIX B

PHOTOGRAPHS OF SAMPLES AFTER TEST
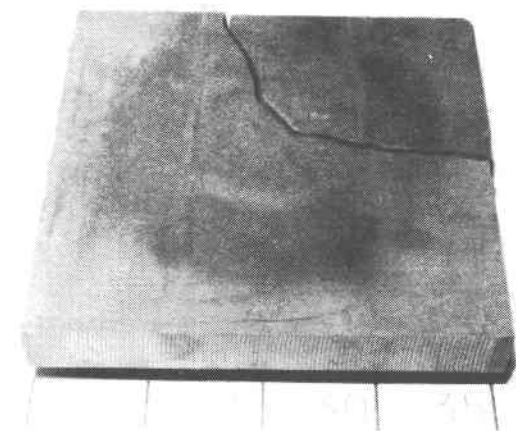
Fig. B-1. Graphite Sample 3499-1

Fig. B-2. Graphite Sample 3499-2
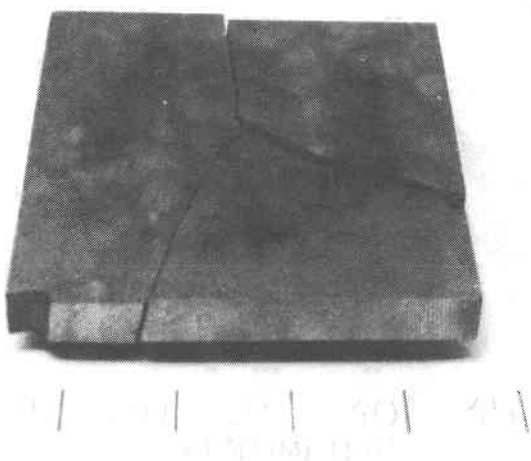
Fig. B-3. Graphite Sample 8826-1
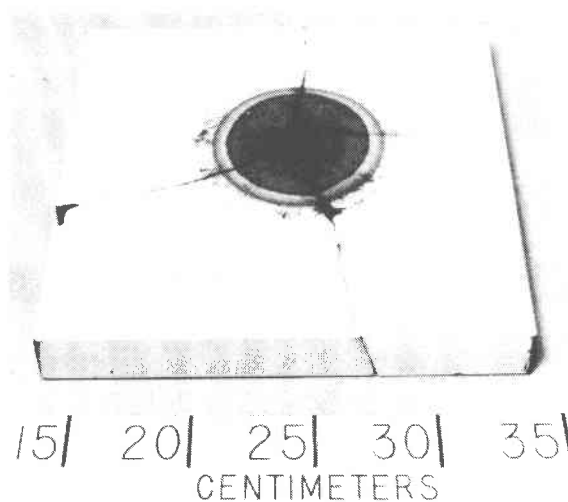
Fig. B-4. Graphite Sample 8826-2
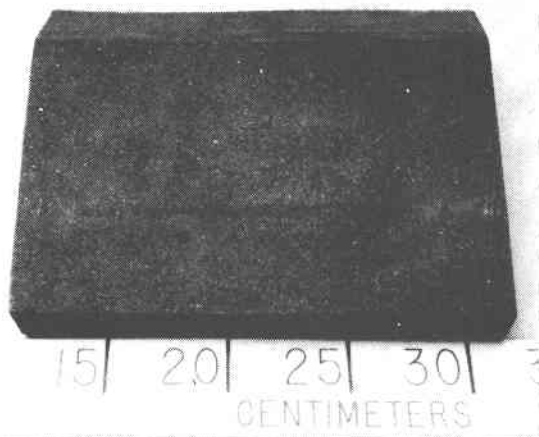
Fig. B-5. Graphite Sample HB-1
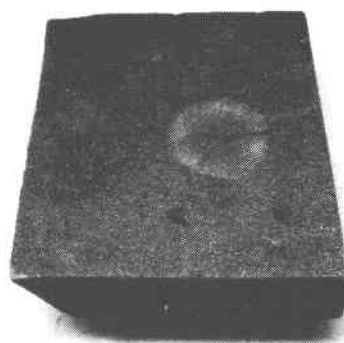
Fig. B-6. Graphite Sample HB-1/2

Fig. B-7. Graphite Sample CS-1
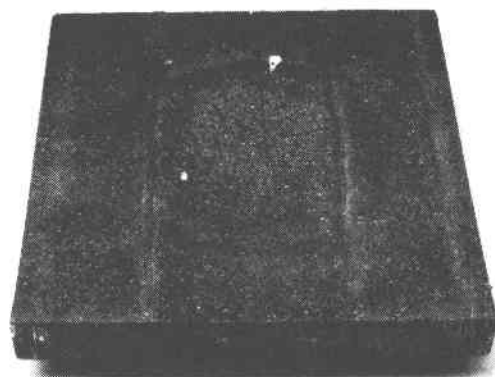
Fig. B-8. Graphite Sample CS-1/2
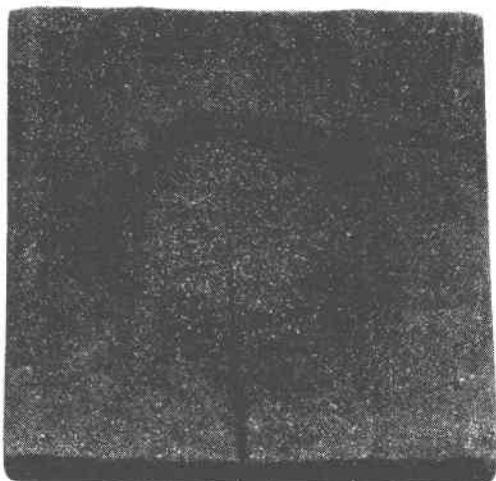
Fig. B-9. Graphite Sample CS-1/4
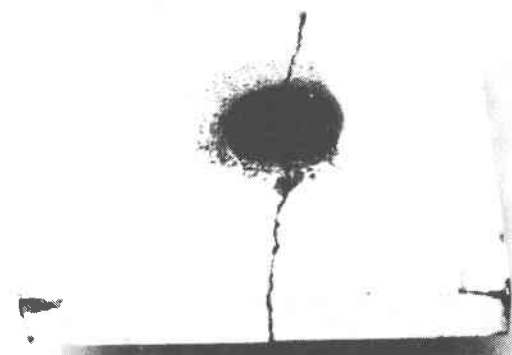
Fig. B-10. Graphite Sample CS-2
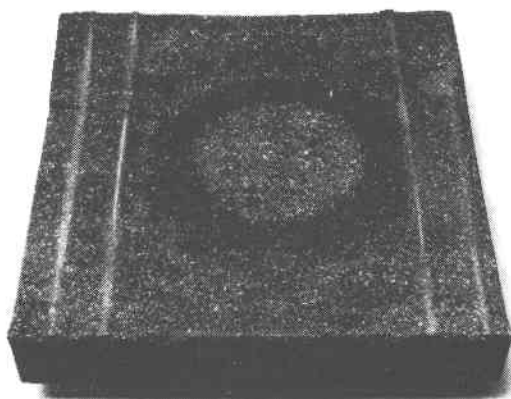
Fig. B-11. Graphite Sample CS-3
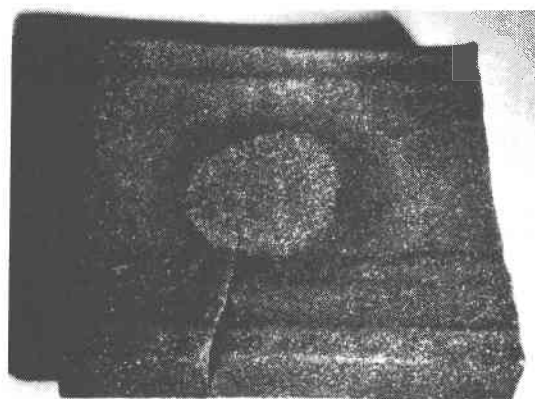
Fig. B-12. Graphite Sample CS-3/2
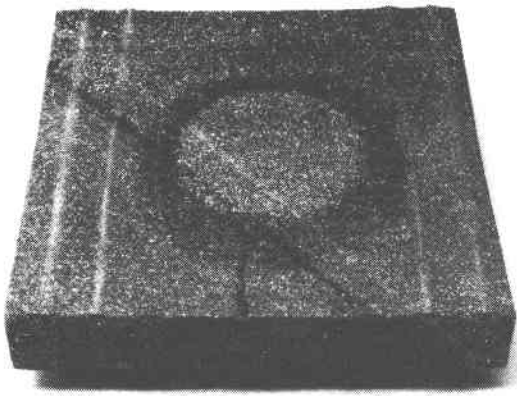
Fig. B-13. Graphite Sample CS-4
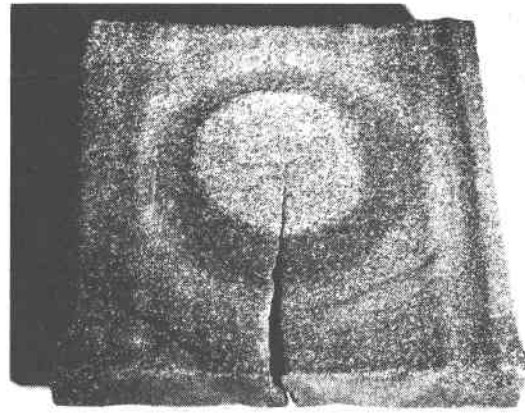
Fig. B-14. Graphite Sample CS-4/2
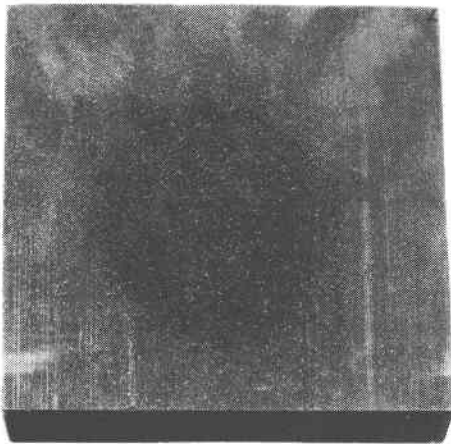
Fig. B-15. Graphite Sample CS-5
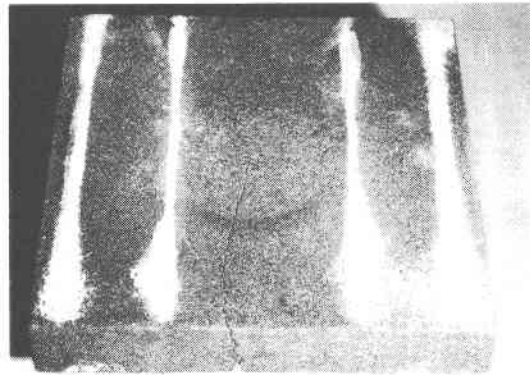
Fig B-16. Graphite Sample CS-6
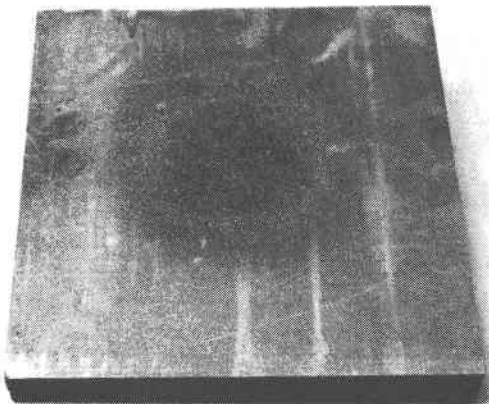
Fig. B-17. Graphite Sample CS-7
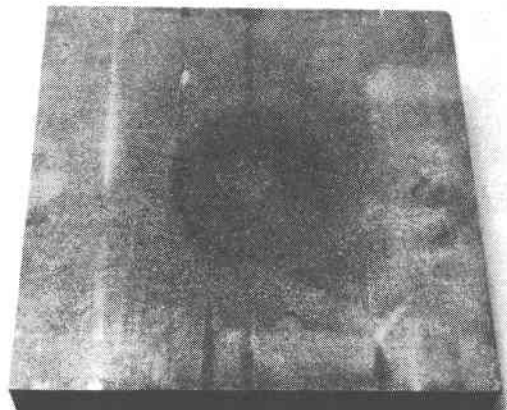
Fig. B-18. Graphite Sample CS-7/2
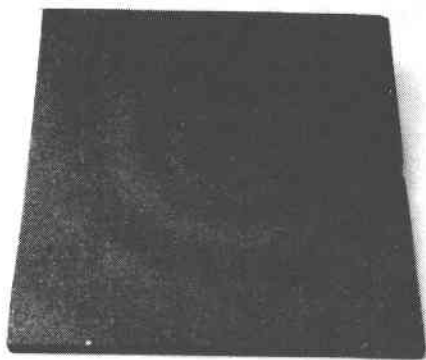
Fig. B-19. Graphite Sample CS-8
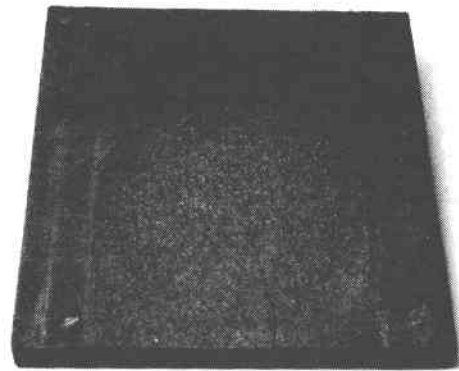
Fig. B-20. Graphite Sample CS-9
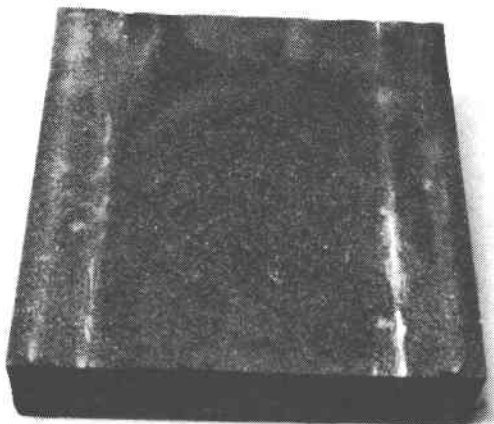
Fig. B-21. Graphite Sample CS-10
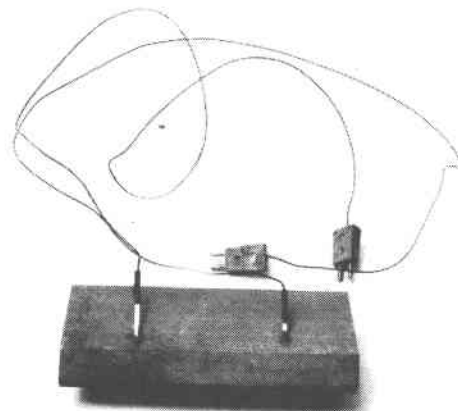
Fig. B-22. Graphite Sample CS-11/2
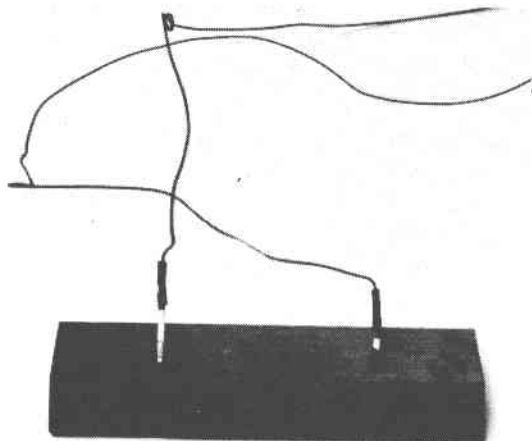
Fig. B-23. Graphite Sample CS-11/3
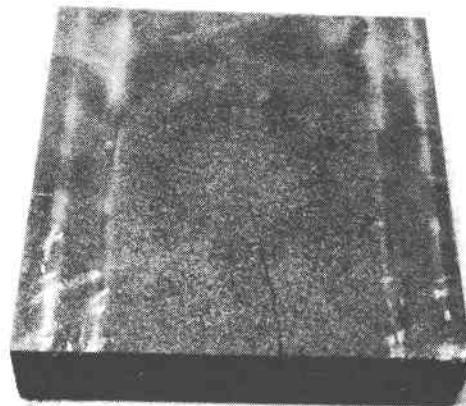
Fig. B-24. Graphite Sample CS-12
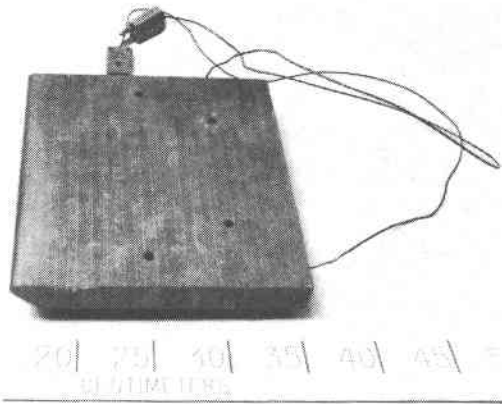
Fig. B-25.   Graphite Sample CS-13/4
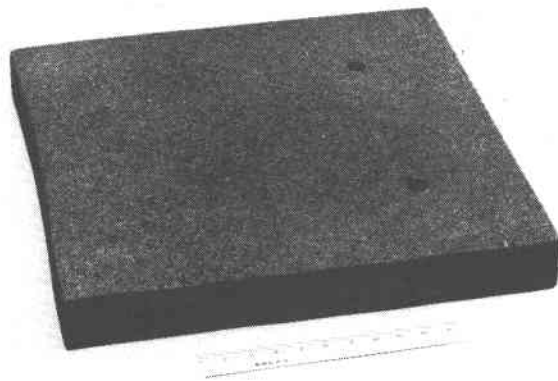
Fig. B-26.   Graphite Sample CS-14/2

Fig. B-27.   Graphite Sample HLM85-1
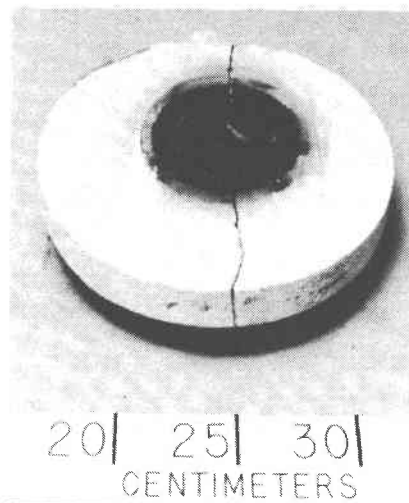
Fig. B-28.   Graphite Sample HLM85-2

Fig. B-29.   Graphite Sample G90-1

Fig. B-30.   Graphite Sample G90-1/2

Fig. B-31.   Graphite Sample G90-2
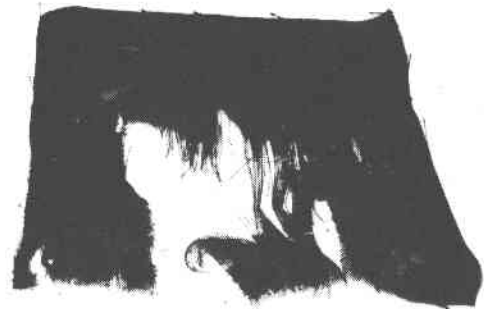
Fig. B-32.   Graphite Sample GPAN-DL-1

1mm
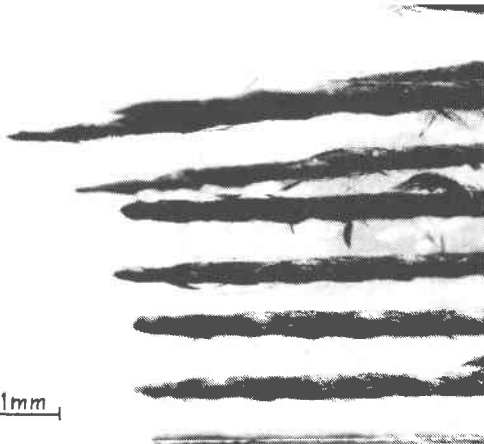
Fig. B-33.   Graphite Sample GPAN-DL-1
(Edge)

Fig. B-34.   Silicon Carbide Sample SiC-1

Fig. B-35.   Silicon Carbide Sample SiC-2
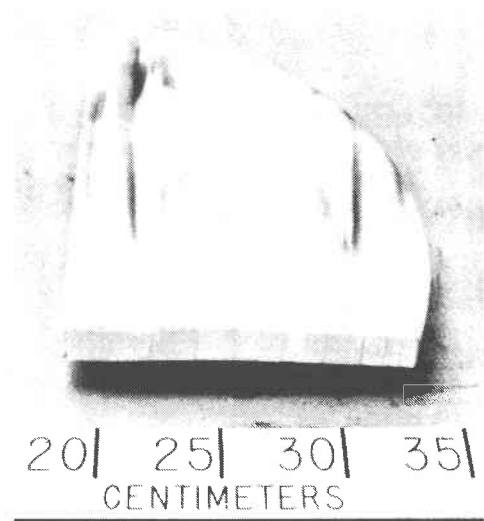
Fig. B-36.   Silica Sample SiO_2-JSS-1
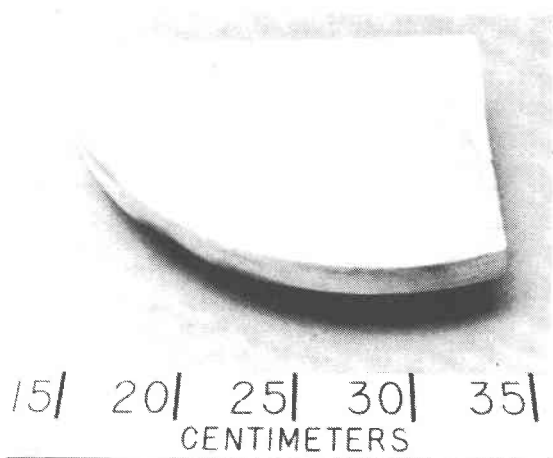
Fig. B-37. Silica Sample SiO_2-JSS-1/2
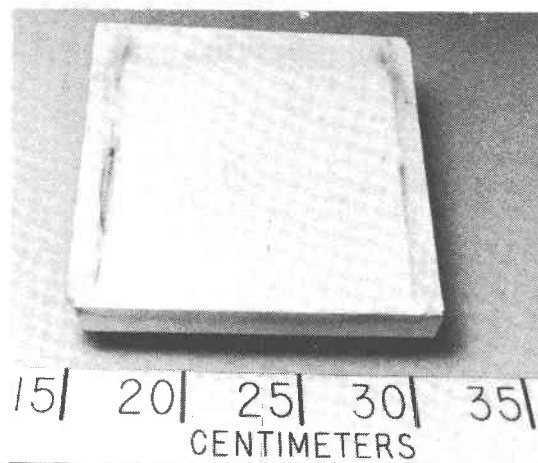
Fig. B-38. Silica Sample SiO_2-JH-1
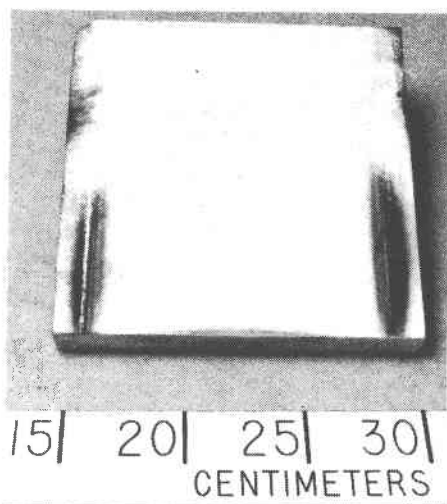
Fig. B-39. Silica Sample SiO_2-JH-1/2
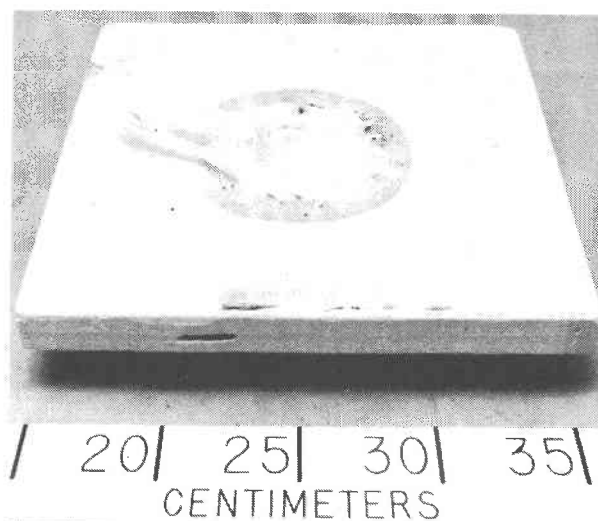
Fig. B-40. Silica Sample SiO_2-DW-2
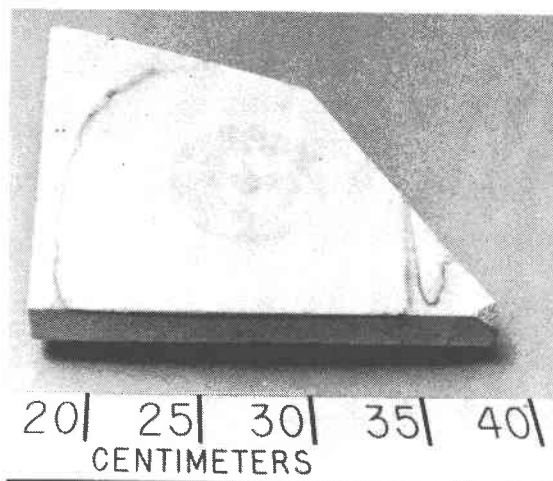
Fig. B-41. Silica Sample SiO_2-DW-4
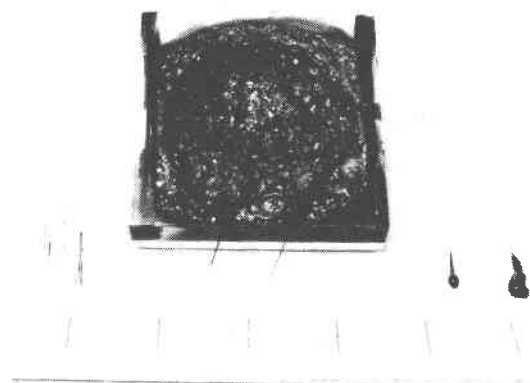
Fig. B-42. Silica Sample $SiO2$-FRCI-12
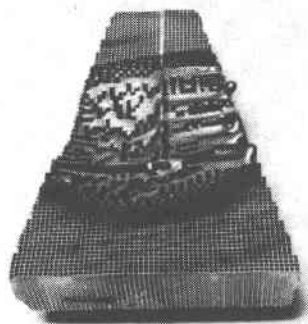
Fig. B-43.   Mullite Sample Mull-1
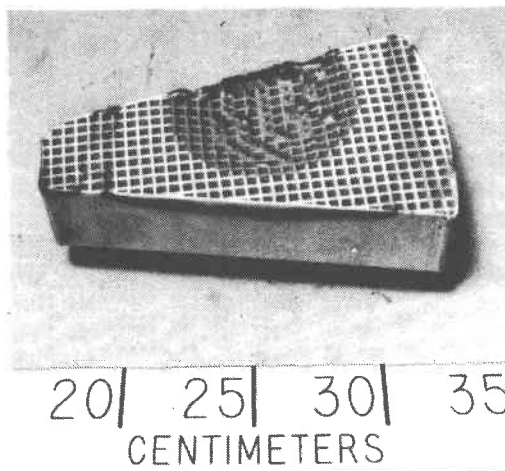
Fig. B-44.   Mullite Sample Mull-2
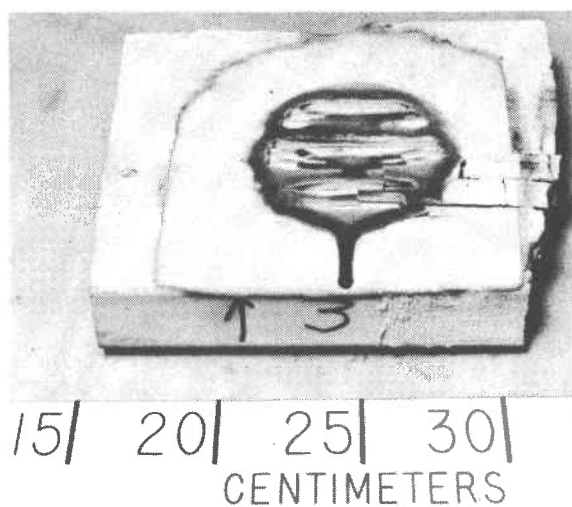
Fig. B-45.   Mullite Sample Mull-3
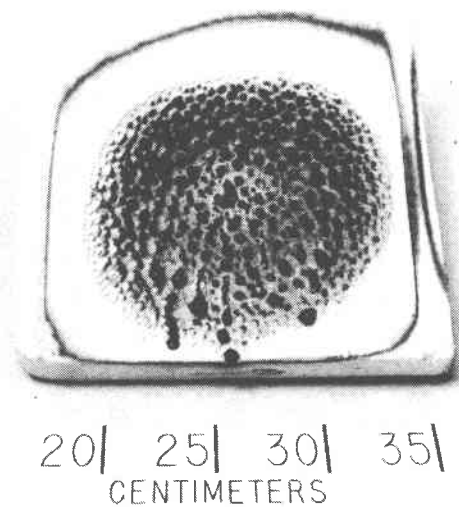
Fig. B-46.   Processed Kaolin Sample WP-1
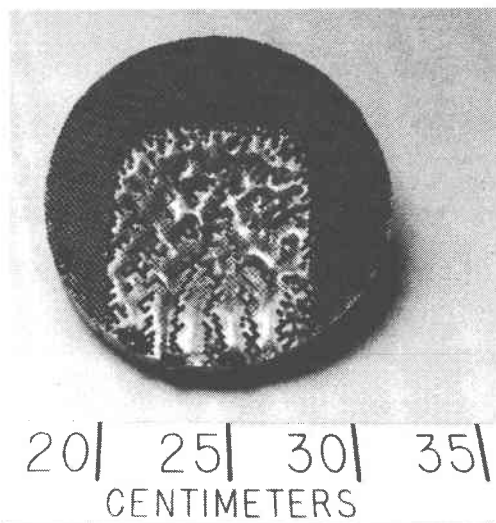
Fig. B-47.   Cordierite Sample CD-MA-1
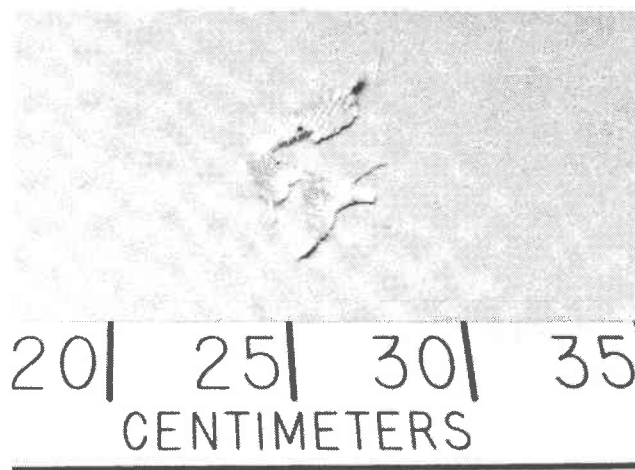
Fig. B-48 Alumina-boria-silica Sample
NT-312-5H-26-1

B-10
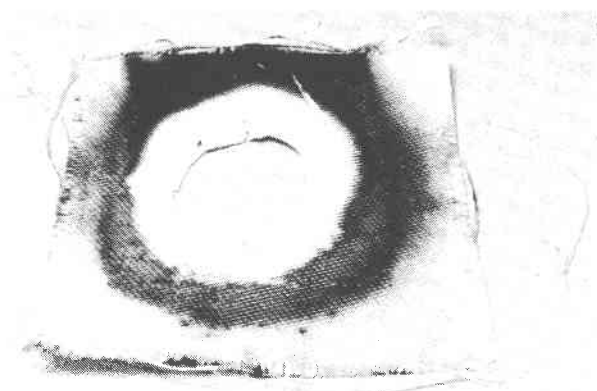
Fig. B-49. Alumina-boria-silica NT-312-5H-40-1
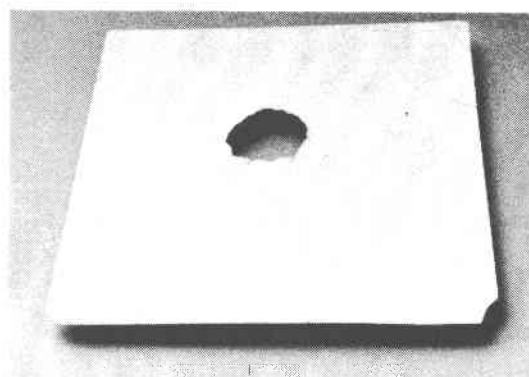
Fig. B-50. Alumina Sample Al_2O_3-1A1
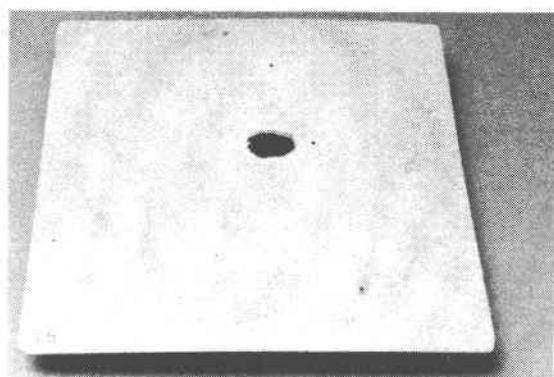
Fig. B-51. Alumina Sample Al_2O_3-1B
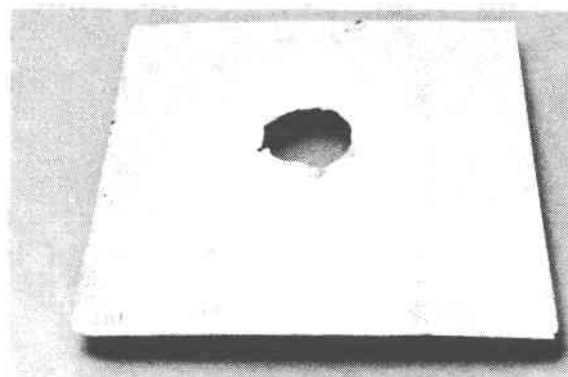
Fig. B-52. Alumina Sample Al_2O_3-2B1
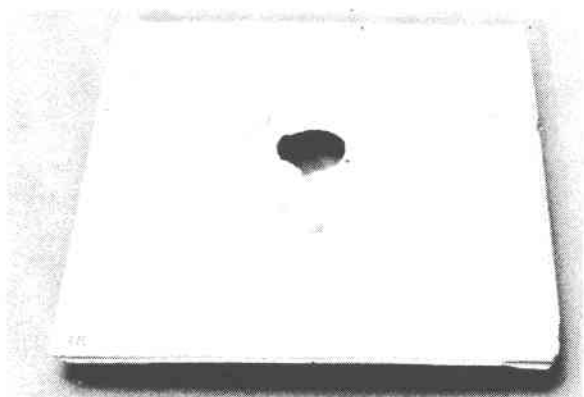
Fig. B-53. Alumina Sample Al_2O_3-3B
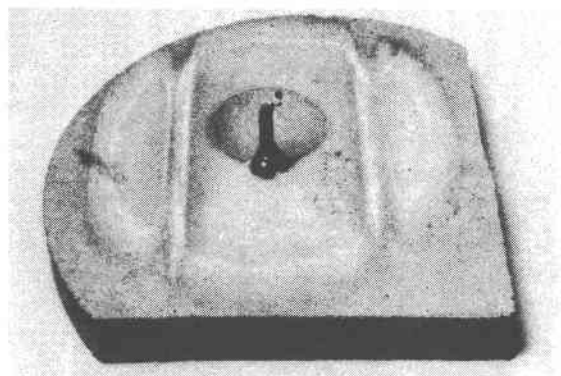
Fig. B-54. Zirconia Sample JSZ-1
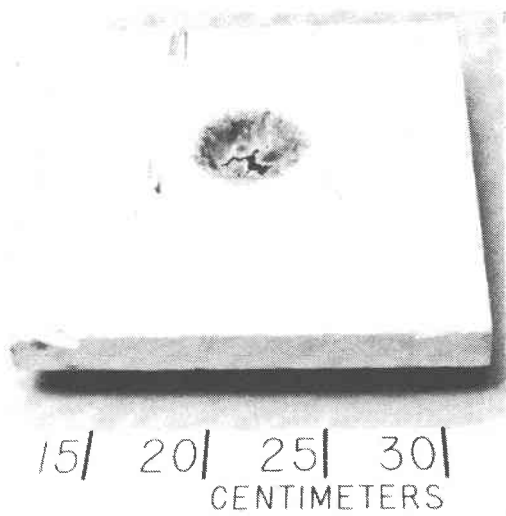
Fig. B-55. Zirconia Sample ZYFB6-1

Fig. B-56. Zirconia Sample ZWY30A-1
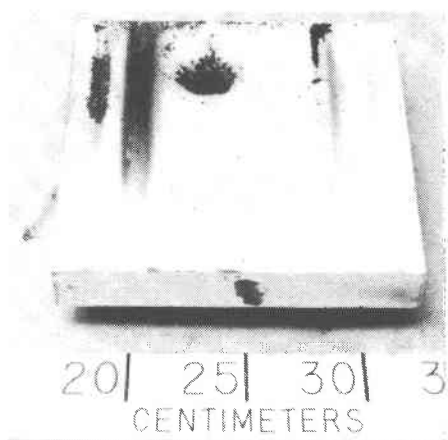
Fig. B-57. Copper Sample Cu-1
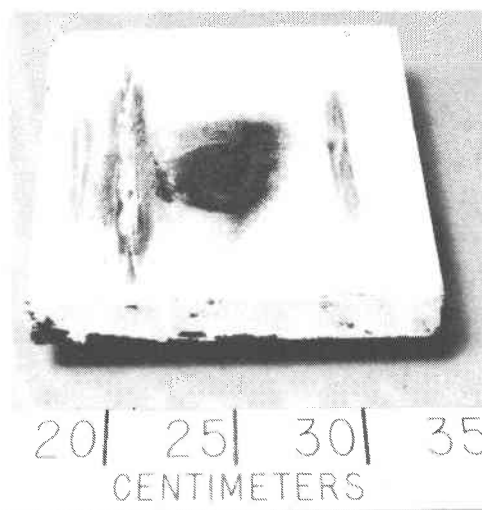
Fig. B-58. Copper Sample Cu-1/2

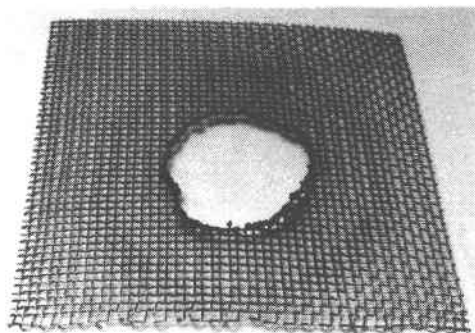Fig. B-59. Copper Sample Cu-1/3
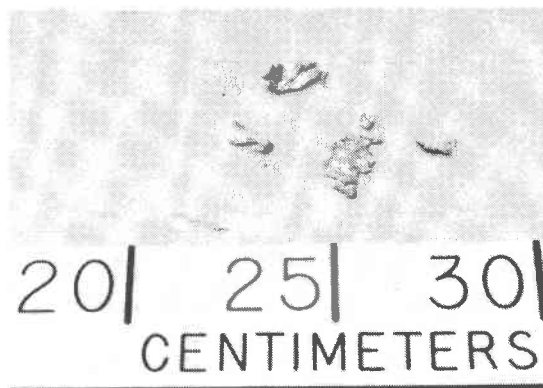
Fig. B-60. Aluminum Sample 18-17

Fig. B-61.   Steel Sample SS-1
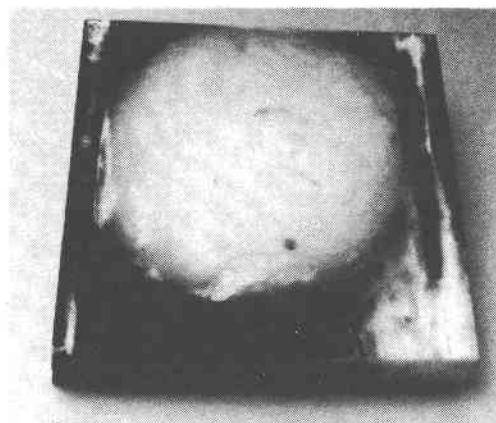
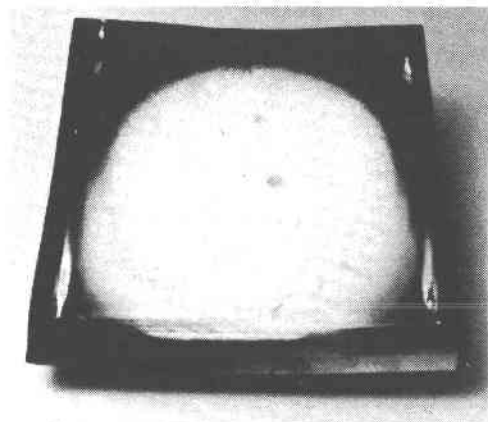Fig. B-62.   Polytetrafluoroethylene
Sample PTFE-1

Fig. B-63.   Polytetrafluoroethylene
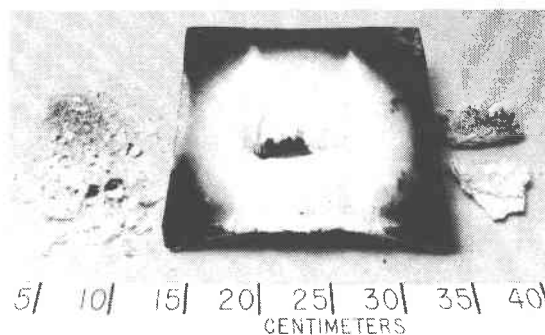Sample PTFE-1/2
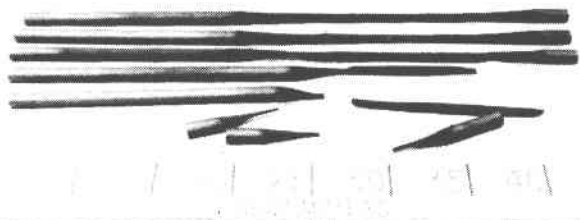

Fig. B-64.   Polytetrafluoroethylene
Sample PTFE-1/3

Fig. B-65.   Support Rods, Graphite
873-S, Used in Tests J-15 and J-16

B-13

UNITED STATES DEPARTMENT OF ENERGY

P.O. BOX 62
OAK RIDGE, TENNESSEE 37830

OFFICIAL BUSINESS
PENALTY FOR PRIVATE USE. $300

```
        10723          FS-  1
US DEPARTMENT OF ENERGY
ATTN  S D ELLIOTT, DIR
SOLAR ONE PROJECT OFFICE
PO BOX 366
DAGGETT, CA      92327
```